

UNCLASSIFIED

AD NUMBER

AD485170

LIMITATION CHANGES

TO:

Approved for public release; distribution is unlimited.

FROM:

Distribution authorized to U.S. Gov't. agencies and their contractors; Critical Technology; JUL 1966. Other requests shall be referred to Army Electronics Command, Attn: AMSEL-HL-CT-R, Fort Monmouth, NJ. This document contains export-controlled technical data.

AUTHORITY

usaec ltr, 27 jul 1971

THIS PAGE IS UNCLASSIFIED

485170

AD



TECHNICAL REPORT ECOM-01711-1

**AUTOMATIC DETECTION AND DISPLAY EQUIPMENT
FOR
MOVING TARGET INDICATION
(ADDEM)**

FIRST QUARTERLY PROGRESS REPORT

BY

L.L. SCHOENFELD

JULY 1966

DISTRIBUTION STATEMENT

This document is subject to special export controls and each transmittal to foreign governments or foreign nationals may be made only with prior approval of CG, U. S. Army Electronics Command, Fort Monmouth, N. J.

Attn: AMSEL-HL-CT-R

ECOM

UNITED STATES ARMY ELECTRONICS COMMAND • FORT MONMOUTH, N.J.

CONTRACT DA 28-043 AMC-01711(E)
GOODYEAR AEROSPACE CORPORATION
ARIZONA DIVISION
LITCHFIELD PARK, ARIZONA

NOTICES

Disclaimers

The findings in this report are not to be construed as an official Department of the Army position, unless so designated by other authorized documents.

The citation of trade names and names of manufacturers in this report is not to be construed as official Government indorsement or approval of commercial products or services referenced herein.

Disposition

Destroy this report when it is no longer needed. Do not return it to the originator.

AUTOMATIC DETECTION AND DISPLAY EQUIPMENT

FOR

MOVING TARGET INDICATION

(ADDEM)

FIRST QUARTERLY PROGRESS REPORT

9 NOVEMBER 1965 TO 31 JANUARY 1966

REPORT NO. 1

CONTRACT NO. DA 28-043 AMC-01711(E)

DA TASK NR. 1P6-20901-A-188-03

PREPARED BY

L. L. SCHOENFELD

GOODYEAR AEROSPACE CORPORATION
ARIZONA DIVISION
LITCHFIELD PARK, ARIZONA

FOR

U.S. ARMY ELECTRONICS COMMAND
FORT MONMOUTH, NEW JERSEY 07703

DISTRIBUTION STATEMENT

This document is subject to special export controls and each transmittal to foreign governments or foreign nationals may be made only with prior approval of CG, U.S. Army Electronics Command, Fort Monmouth, New Jersey
ATTN: AMSEL-HL-CT-R

TABLE OF CONTENTS

	<u>Page</u>
LIST OF ILLUSTRATIONS	iii
LIST OF TABLES	iv

<u>Section</u>	<u>Title</u>	
I	PURPOSE	1
II	ABSTRACT	3
III	FACTUAL DATA	5
	1. Introduction	5
	2. Active Filters	5
	3. Storage-Display Tube	14
	4. High-Voltage Power Supply	14
	5. Voltage Regulator	18
	6. Integrator-Threshold Circuits	23
	7. Integration Technique	26
	8. Radar Simulator	26
IV	CONCLUSIONS	31
	LIST OF REFERENCES	33

Appendix

A	HUMAN FACTOR ENGINEERING SELECTION CRITERIA FOR AZIMUTH-RANGE DISPLAY	35
B	AN ALGORITHM FOR THE COMPUTATION OF FIRST PROBABILITY DENSITIES AT THE OUTPUT OF A LINEAR FILTER FOR A NON- GAUSSIAN INPUT	37
C	DERIVATION OF ACTIVE FILTER TRANSFER FUNCTION	45

LIST OF ILLUSTRATIONS

<u>Figure</u>	<u>Title</u>	<u>Page</u>
1	Prototype Passive Filter	9
2	Response Characteristics of Bandpass Filters	11
3	Active Filter Realization	12
4	Response of Test Circuit	13
5	High-Voltage Power Supply Test Circuit Simplified Schematic Diagram	16
6	Construction Details of Variable Transformer	17
7	Voltage Regulator Schematic Diagram	19
8	Voltage Regulator Waveforms	22
9	Integrator-Threshold Test Circuit Schematic Diagram	24
10	Integrator-Threshold Circuit Timing Diagram	25
11	Target Simulator Schematic Diagram	27
12	Radar Simulator Waveforms	30
B-1	Detection Probabilities for Noise Only and Signal Plus Noise . . .	37
B-2	Basic System	38
C-1	Generalized Configuration	45

LIST OF TABLES

<u>Table</u>	<u>Title</u>	<u>Page</u>
I	Pole Location for Bandpass Filters	10
II	Regulator Efficiency	21

SECTION I - PURPOSE

The purpose of this program is to develop, fabricate, and test an Automatic Detection and Display Equipment for Moving Target Indication. This equipment will be used in conjunction with battlefield surveillance radars such as the AN/TPS-25, AN/TPS-33, and AN/PPS-5 to detect moving targets and display them on a range versus azimuth display.

The more pertinent design requirements are:

1. Ten range-gated channels, each containing ten each bandpass filters, detectors, integrators, threshold circuits, and indicators. The range gates will be either 50 or 100 m in width and the range gated interval will be adjustable in range between 0 and 9500 m.
2. A range versus azimuth display to indicate the doppler frequency and range of a detected moving target. A total of 100 indicators will monitor 10 frequency channels in each of the 10 range gates.
3. A range versus azimuth indicator to present the operator with a B-scope display. This indicator will have a persistence variable between 1 second and 30 minutes and will present only moving targets.
4. A volume of less than 1 cu ft, weigh less than 25 lb. and consume less than 25 w of power.
5. Operation under rigorous field conditions.

More detailed specifications can be obtained from Electronics Command Technical Requirement SCL-8029.

This program is being conducted under Contract Number DA28-043-AMC-01711(E) ending 30 April 1967, with the delivery of one fully tested detection and display unit.

Credit must be given to B. Wood and D. O'Herren who collaborated in writing the section on active filters, P. Resta who prepared Appendix A, and R. Ford for the work in Appendix B.

SECTION II - ABSTRACT

This is the first quarterly report documenting the development of an Automatic Detection and Display Equipment for Moving Target Indicator (MTI).

An investigation of active filters was undertaken and a preliminary configuration selected for test. This circuit makes use of integrated operational amplifiers. In addition, the S-plane pole position for all 10 bandpass filters was calculated.

Effort was also expended on development of a +10,000-vdc power supply for the storage-display tube. A 10-kHz solid-state inverter driving voltage multipliers and rectifiers was selected for test. A small variable transformer was also developed to provide highly efficient adjustment of voltages.

An input voltage regulator was developed and, through use of a special configuration, a regulating efficiency of 95 percent was achieved. Other development work consisted of preliminary test of an integrator-threshold circuit and the target generator and doppler modulator portion of a radar simulator.

SECTION III - FACTUAL DATA

1. INTRODUCTION

This report describes the initial effort expended toward development of an Automatic Detection and Display Equipment for Moving Target Indication. During this reporting period, the primary emphasis was directed toward proving the feasibility of techniques employed in the original system concept. Parametric analysis and circuit development were conducted in seven basic areas. These are:

1. Active filter investigation
2. Storage-display tube
3. High-voltage power supply
4. Voltage regulator
5. Integrator-threshold circuit
6. Integration technique
7. Target simulator.

No separate effort was conducted toward reduction of size, weight, or power consumption. Rather, all work was conducted with these considerations as prime goals.

2. ACTIVE FILTERS

The effort expended on design of the bandpass filters has been largely analytical. Before synthesis could be undertaken, it was necessary to determine where the poles of the response function were located. Texts in network synthesis exist which discuss the Tschebyscheff function thoroughly. However, the tabulated values and methods of synthesis given invariably refer to a method of obtaining the element values for a normalized low-pass prototype. This function has not proven to be the required function; first because of the normalization and, second, and more important, because of the frequency transformation between the low-pass prototype and the required bandpass function.

The method which has finally resulted in the desired pole positions is summarized below.

Given that it is desired to obtain the pole locations for a bandpass filter with specified response characteristic across the passband and specified rate of attenuation outside the passband, the following approach will directly produce the desired locations with a nominal amount of effort.

The first step involves determining poles of the low-pass prototype filter; it is followed by sliding the poles, in the S plane, to the appropriate location for the particular passband. This produces a normalized filter in terms of R's, L's, and C's as well as the

desired pole locations. The low-pass prototype may have a Butterworth frequency response characteristic or an equiripple Tschebyscheff characteristic.

In either case, one begins with a typical low-pass filter shown in Figure 1(A) and derives the transfer function

$$\frac{E_o}{E_i} = \frac{\frac{R}{RCS + 1}}{LS + \frac{R}{RCS + 1}} = \frac{R}{LRCS^2 + LS + R} = \frac{1}{LCS^2 + \frac{L}{R}S + 1} = \frac{1}{(S - S_1)(S - S_1^*)} \quad (1)$$

where S_1, S_1^* are the complex roots of the denominator polynomial. For this particular transfer function,

$$S_1, S_1^* = \frac{1}{2LC} \left[-\frac{L}{R} \pm j \sqrt{4LC - \left(\frac{L}{R}\right)^2} \right]. \quad (2)$$

It follows that specifying the real and imaginary parts of S_1, S_1^* defines the R, L , and C of the low-pass prototype.

The following will describe the technique used for a Tschebyscheff two-pole bandpass filter with maximum ripple of 1 db where the bandpass of interest may be as low as 30 to 50 Hz and as high as 1400 to 1600 Hz.

It has been thoroughly documented^{1a} that the poles of a normalized Butterworth filter lie equally spaced on a unit circle. For the two-pole case, see Figure 1(B). It is further documented that poles of a Tschebyscheff filter, having an equiripple

^{1a} Superior numbers in the text refer to items in the List of References.

characteristic in its otherwise equivalent passband, have a direct correspondence to the Butterworth poles. Thus, the Tschebyscheff poles may be found from the Butterworth pole locations by reducing the negative real coordinate by a factor γ defined by the desired passband ripple characteristic (Figure 1(C)). Thus, if the unit circle is considered to have radius $\cosh \gamma$, the Tschebyscheff poles will lie on an ellipse having minor axis $\sinh \gamma$.

$$\gamma = \frac{1}{n} \sinh^{-1} \frac{1}{\sqrt{\epsilon}} \quad (3)$$

where n is the number of desired poles and ϵ the passband ripple factor.

The effort required to obtain the S-plane poles of low-pass prototype filter for a given passband characteristic is not great. However, it is far simpler to use the excellent tables of S-plane pole locations found in Weinberg².

Given the low-pass prototype pole locations which define the R, L, and C of Figure 1(A), it remains to slide these to a particular passband. Begin by extending the low-pass filter from its normalized cutoff at $W_c = 1$ to a W_c equivalent to the desired passband width. Next, determine the nominal center of the desired passband

$$W_o^2 = W_1 W_2 \quad (4)$$

where

$$W_1 = 2\pi f_1 \text{ and } W_2 = 2\pi f_2.$$

f_1 and f_2 are the extremes of the desired passband in Hz. The object now is to resonate each of the reactive elements of the extended low-pass prototype with a complementary element at this desired center. In effect, each of the resonating pair of elements of the extended low-pass filter is converted to a new pair of elements resonating at W_o . In brief,

$$\begin{aligned} W_{PB} &= W_2 - W_1 \\ L_1 &= \frac{L}{W_{PB}} & C_1 &= \frac{C}{W_{PB}} & R_1 &= R \\ C'_1 &= \frac{1}{W_o^2 L_1} & L'_1 &= \frac{1}{W_o^2 C_1} \end{aligned} \quad (5)$$

Figure 1(D) represents the realization of the desired passband filter with specified Tschhebyscheff passband characteristic.

The transfer function of this realization is evaluated as

$$\frac{e_o}{e_i} = \frac{\frac{s^2}{L_1 C_1}}{s^4 + \frac{s^3}{RC_1} + s^2 \left[\frac{1}{L'_1 C_1} + \frac{1}{L_1 C'_1} + \frac{1}{L_1 C_1} \right] + \frac{s}{L_1 C'_1 RC_1} + \frac{1}{L_1 C'_1 L'_1 C_1}} \quad (6)$$

To realize this function by active synthesis methods, it is necessary to know the pole locations which are the roots of the denominator function. These roots have been solved on the 1620 computer and are tabulated in Table I, along with the required center frequencies and damping factors, or Q's.

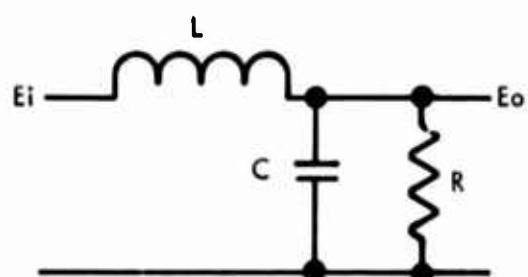
From these pole locations, the response functions of the entire set of filters are shown in Figure 2.

There are various possible configurations which could be used in building the required filter systems. The first considered was a purely passive network, and a request for quotes produced a response which indicated that both weight and volume requirements would be exceeded if the entire set of filters were realized by this means. However, at this time, it still appears that a combination of passive, high-frequency filters could be used with an active realization of the lower frequency types where inductor size and weight are excessive.

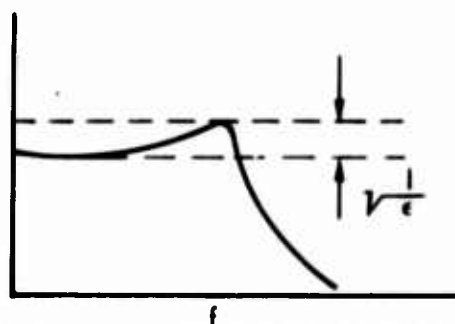
Of the various active filters, one, about which considerable literature exists, is the negative impedance converter^{3, 4}. It appears that its principal limitation is that of gain stability with environmental changes. As a result, this filter realization is not presently under consideration.

Another active filter type is the low-pass, high-pass configuration of an emitter follower^{5, 6, 7}. This filter appears to offer some possibilities, but further research is necessary before a decision is made.

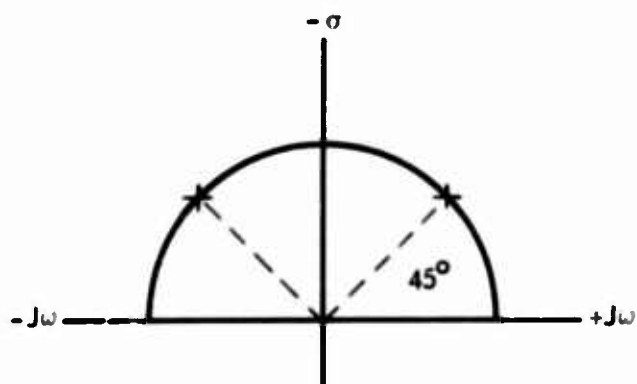
The method of realization currently under investigation is that of using a high-gain amplifier with a negative feedback network around it to realize a desired transfer function. This is essentially the method indicated in the proposal supplement except that the amplifiers currently under evaluation are high-gain operational types made with integrated circuitry. The recent introduction of low-cost, high-gain silicon



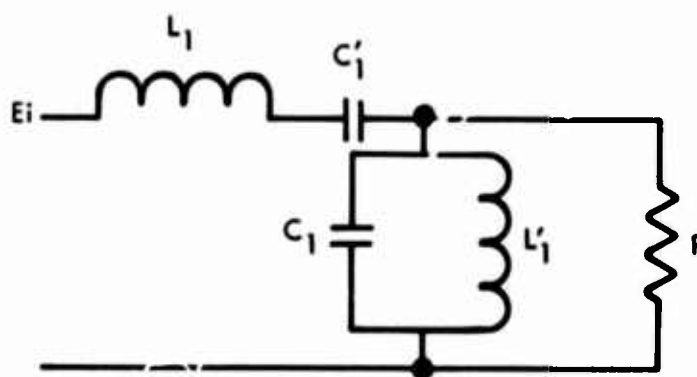
(A) LOW-PASS PROTOTYPE FILTER



(C) THE TSCHEBYSCHIEFF RIPPLE FUNCTION



(B) POLE LOCATION FOR A TWO-POLE BUTTERWORTH FUNCTION



(D) BANDPASS REALIZATION

4039-9

Figure 1 - Prototype Passive Filter

TABLE I - POLE LOCATION FOR BANDPASS FILTERS

Passband (H _z)	Pole locations (radians/second)	ω_n	ζ	Q
30 to 50	26.649362 \pm j191.25075 42.323325 \pm j303.73600	193.0985185 306.6705423	0.138009 0.138009	3.6229
50 to 100	59.78927 \pm j318.11725 112.64244 \pm j599.33020	323.6871044 609.8237515	0.184713 0.1847133	2.7069
100 to 200	119.57852 \pm j636.23450 225.28490 \pm j1198.6603	647.3742050 1219.647408	0.1847131 0.1847131	2.7069
200 to 400	239.15706 \pm j1272.4689 450.56975 \pm j2397.3206	1294.748315 2439.294807	0.1847131 0.1847131	2.7069
400 to 600	282.50972 \pm j2548.2171 407.21713 \pm j3673.0689	2563.829583 3695.573153	0.1101905 0.1101905	4.5374
600 to 800	300.53938 \pm j3813.5308 389.18748 \pm j4938.3825	3825.355026 4953.69444	0.078565 0.078565	6.3641
800 to 1000	310.45803 \pm j5075.0655 379.26882 \pm j6199.9173	5084.552488 6211.508010	0.061059 0.061059	8.1888
1000 to 1200	316.74212 \pm j6334.8405 372.98473 \pm j7459.6922	6342.754112 7469.011000	0.0499376 0.0499376	10.0126
1200 to 1400	321.08239 \pm j7593.6576 368.64446 \pm j8718.5094	7600.442726 8726.299610	0.042245 0.042245	11.8357
1400 to 1600	324.26076 \pm j8851.8968 365.46609 \pm j9976.7485	8857.833933 9983.440092	0.036607 0.036607	13.6585

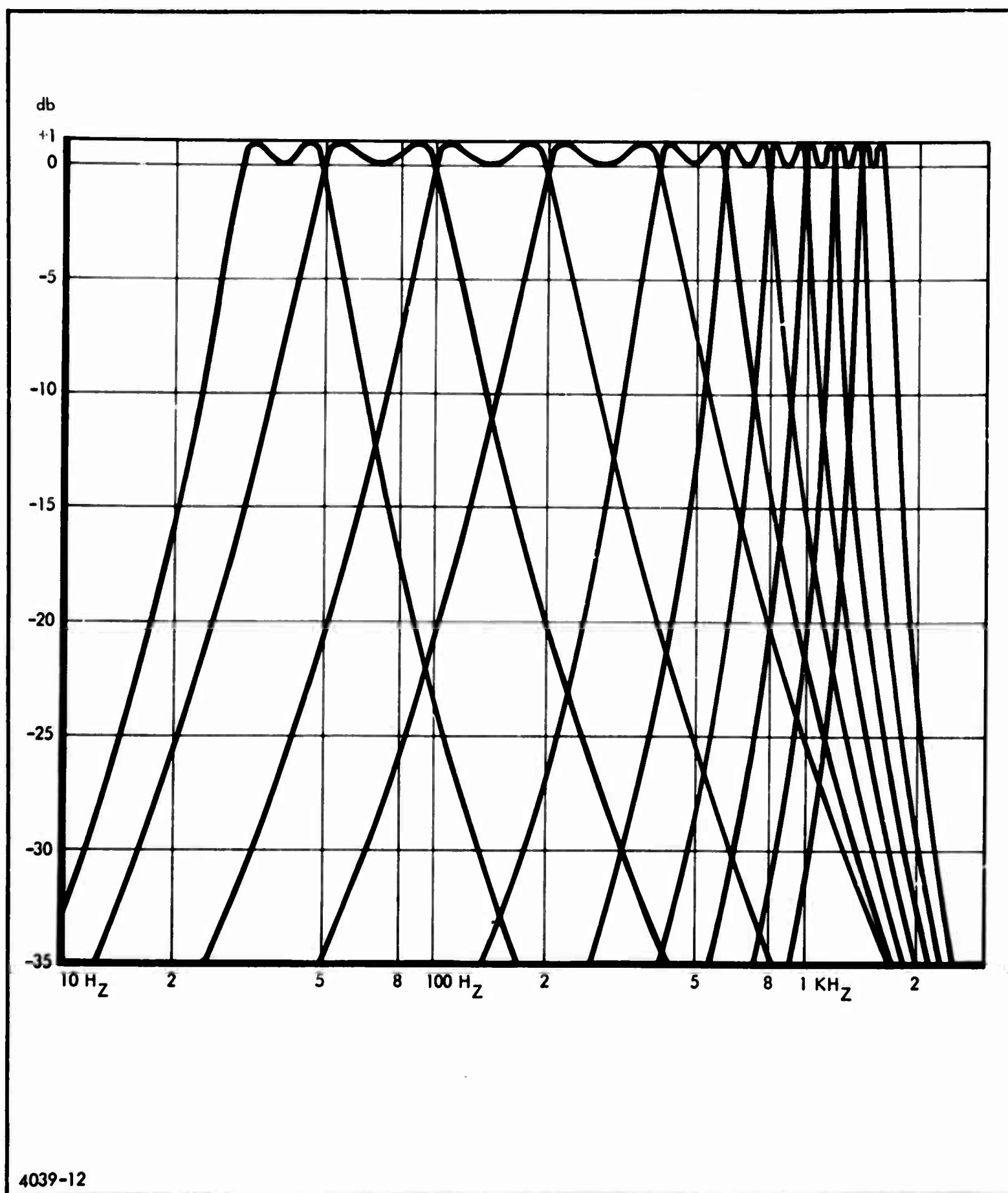


Figure 2 - Response Characteristics of Bandpass Filters

monolithic amplifiers, with typical open-loop gains of 60 db, have made this approach appear desirable from several standpoints. First, the size of these amplifiers is small enough to produce an advantage in packaging, and, second, the high open-loop gain makes the realization of these filters, with the specified accuracy and tolerance, look much more feasible. Also, the high gain with high-negative feedback should make the closed-loop gain much less dependent upon the environment.

Figure 3(A) shows the basic circuit configuration. The transfer function (see Appendix C) is

$$\frac{E_o}{E_i} = - \frac{R_1 C_2 S}{R_1 R_2 C_1 C_2 S^2 + S C_1 (R_1 + R_2) + 1} \quad (7)$$

assuming the gain of the amplifier is a very high negative number. Therefore, since it is possible to factor the denominator function into two complex conjugate roots, this circuit will realize one of the poles used in building a two-pole Tschebyscheff. Two circuits in cascade will realize one filter function, as shown in Figure 3(B).

The response of the two amplifiers in cascade is shown plotted in Figure 4. This essentially realizes the 30- to 50-cycle bandpass figure.

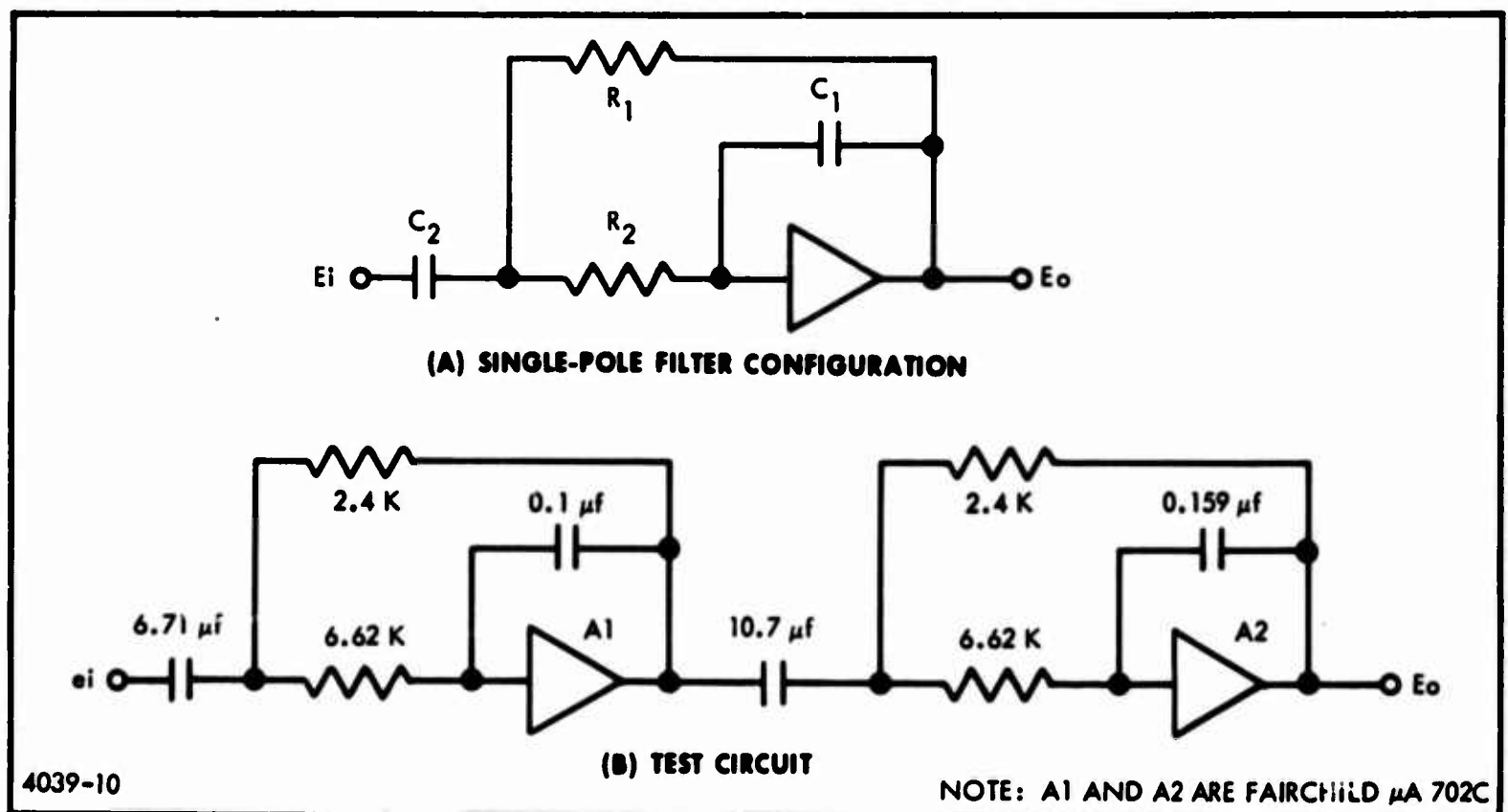


Figure 3 - Active Filter Realization

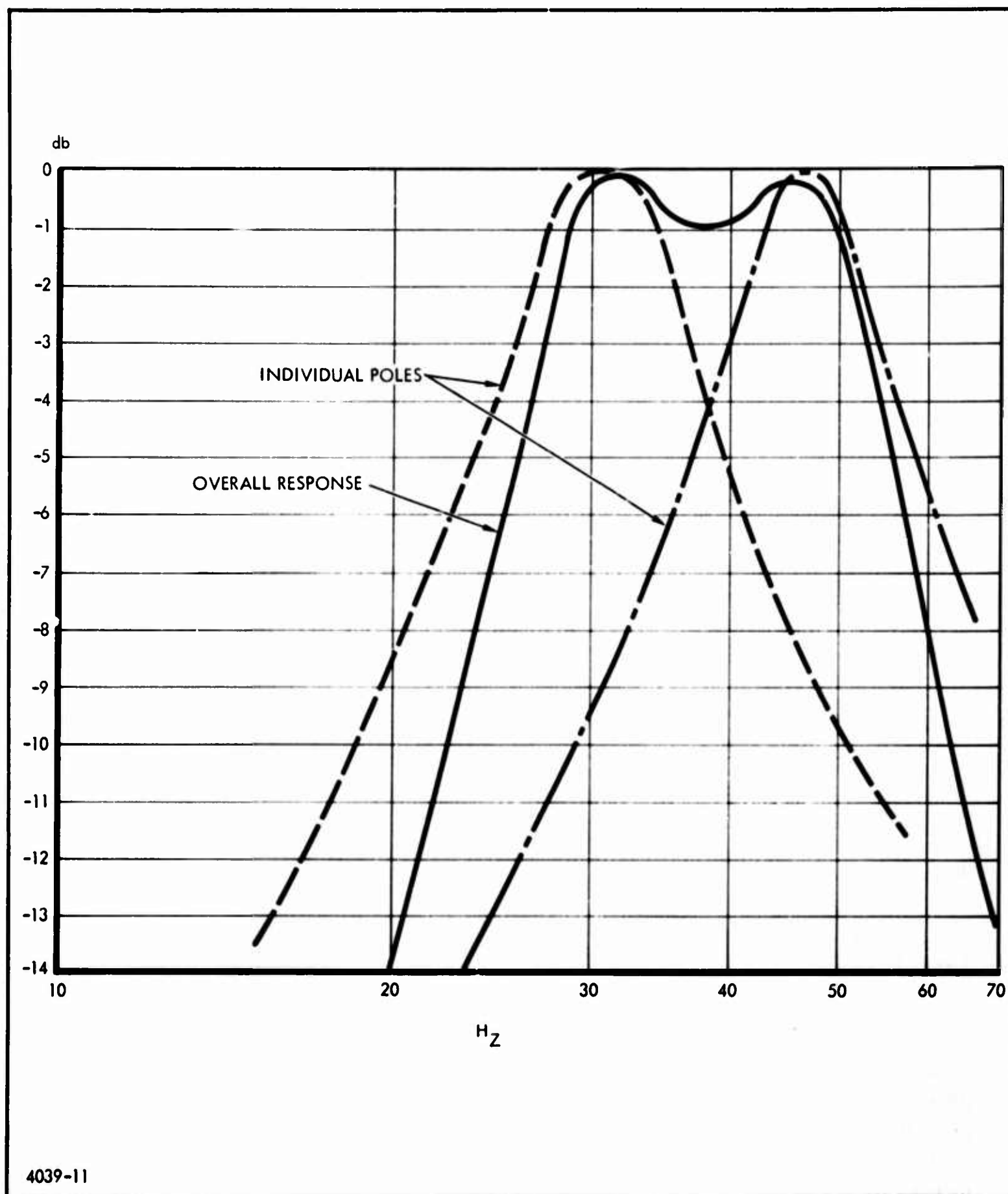


Figure 4 - Response of Test Circuit

3. STORAGE-DISPLAY TUBE

An investigation was undertaken to determine the storage-display tube most suitable for use as a range-azimuth indicator. A great number of different devices of this type are available, but only two types meet the requirements for this application. The type H-1102AP20 Tonotron, manufactured by Hughes Aircraft Company, Vacuum Tube Products Division, has been selected. A special version of this tube, modified for minimum power consumptions, will be designated the H-1192.

This tube is a 5-in. electrostatically deflected device with a weight of approximately 3 lb and packaged for use in severe environments. A useful screen diameter of 3.0 in. will allow a raster 3.5 in. in azimuth and 2 in. in range. For 300 elements in the azimuth direction and 50 in the range direction, a single target will have the dimensions of 0.011 in. in azimuth and 0.04 in. in range. The H-1192 tube has sufficient resolution (85 lines per inch) to achieve this condition.

The most critical aspect concerning the storage display tube is the requirement for 30-minute storage time. Hughes engineers report achieving 30-minute storage time with a final intensity of 50-ft-L. Appendix A indicates an intensity of between 100 and 20 mL (1 ft-L \approx 1 mL) is required for good detection capability. (Appendix A also points out the necessity of considering operator visual adaptation and contrast ratio when determining the acceptability of a display of this type.) More exact data cannot be obtained until a tube is received and tested under actual operating conditions.

4. HIGH-VOLTAGE POWER SUPPLY

The design of a high-voltage power supply with outputs up to 10,000 v and several adjustable voltages represents a difficult engineering task. When maximum efficiency and minimum size and weight are also required, standard techniques cannot be used and new ones must be developed. Progress, to date, is extremely encouraging and will be discussed in some detail.

The three aspects which were judged to be most difficult received the initial effort. These are: an extremely efficient magnetic multivibrator, the 10,000-v supply, and a low-loss method for adjusting voltages. The first two are interdependent since both are based on the transformer design.

This transformer has many conflicting requirements and an optimum compromise is difficult. The final configuration has not been achieved, but tests to date are encouraging. It appears that a small core of square-loop material, such as Deltamax with a moderate number of primary turns, will give the most efficient design. The square-loop material ensures minimum surge current during transistor switch over, and the

moderate number of primary turns reduces the magnetizing current. The secondary winding must be tightly coupled to the core to reduce leakage inductance and care must be taken to reduce the secondary capacitance to ground. Since the capacitance is determined by the length of wire in the secondary winding, rather than by the number of turns, the small core will reduce capacitance. The present configuration has 94 turns primary (collector-to-collector) and 6580 turns in the secondary to provide a secondary voltage of 1250 v.

Because tight coupling to the core is necessary for the secondary, insulation becomes a distinct problem. For this reason, and because of the capacity, the output voltage of 1250 v has been chosen. To achieve the higher voltages, capacity driven voltage multipliers will be used. The configuration is shown in Figure 5. Tests have been made on a circuit of this type to achieve an output of +5000 v. No difficulties are anticipated in doubling the number of rectifier bridges and coupling capacitors to achieve the required 10,000 v.

The use of square waves to drive the rectifiers is highly advantageous. Almost pure dc is obtained directly from the rectifiers without filtering. This will not only save weight but also reduce the hazard to maintenance personnel. It does, however, require the use of special high-speed diodes in the rectifiers.

The use of a small core and voltage multipliers to achieve high voltages seems to offer substantial advantages in size and weight when compared to direct transformation and a single rectifier. Consider, for example, the difficulty that would be encountered in fabricating a transformer to couple 10 kHz square waves using a secondary of 94,000 turns insulated to withstand 10,000 v.

The storage display tube that is to be used for the range-azimuth display requires four and perhaps five adjustable voltages. These are listed below:

1. Write gun grid -2050 to 2090 v
2. Write gun focus +350 to +750 v
3. First collimating electrode +20 to +35 v
4. Second collimating electrode +35 to +70 v

It may also be necessary to adjust astigmatism. Obtaining these variable voltages with potentiometers in a voltage divider would waste considerable power. To preclude incurring this waste, a small variable transformer has been developed.

The construction of this variable transformer is shown in Figure 6. A small toroidal core is wound with a single layer of wire, closely spaced on the inside of the core. Insulation is removed from the outer surfaces of wires in the core center and a carbon brush is

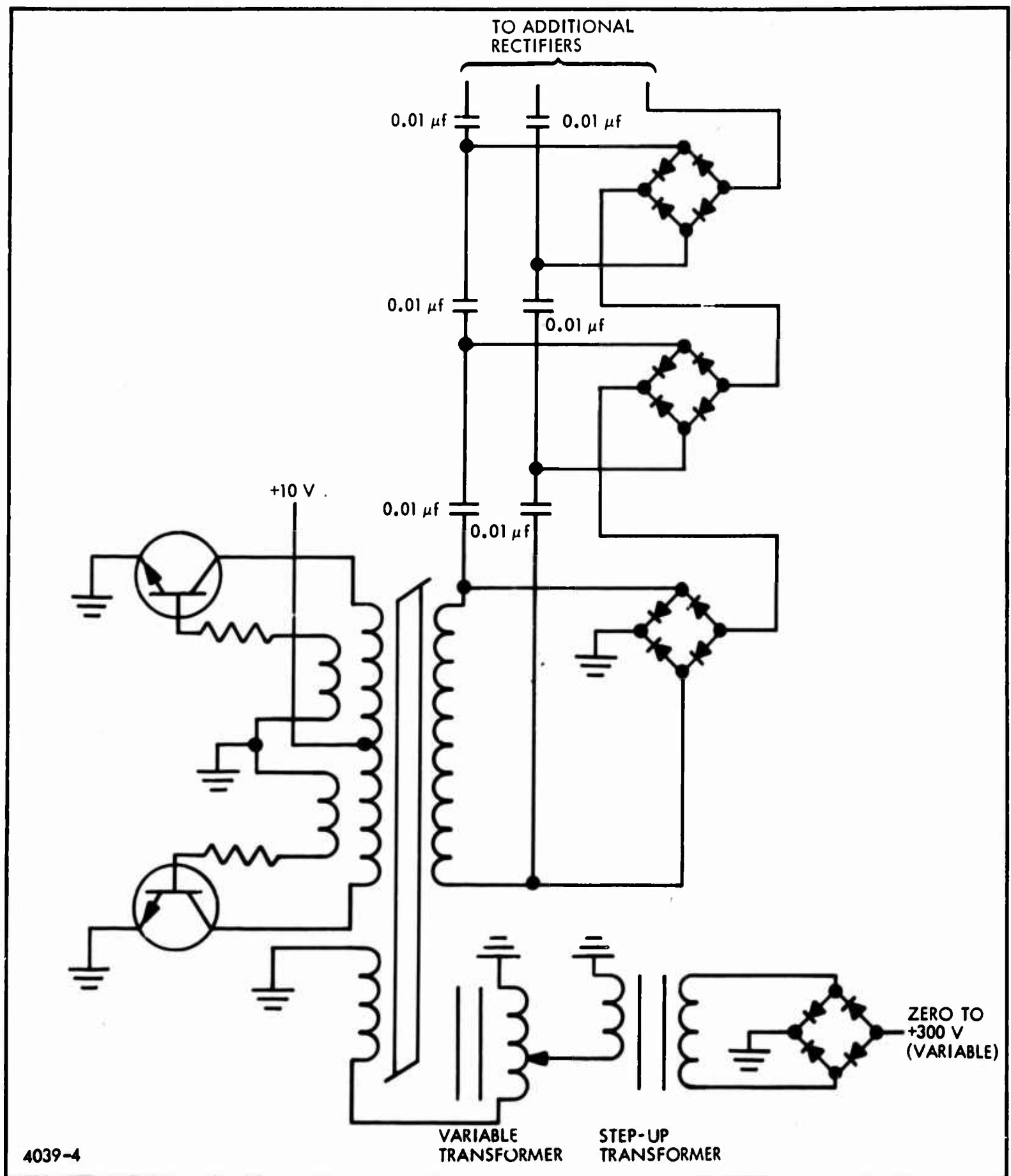


Figure 5 - High-Voltage Power Supply Test Circuit Simplified Schematic Diagram

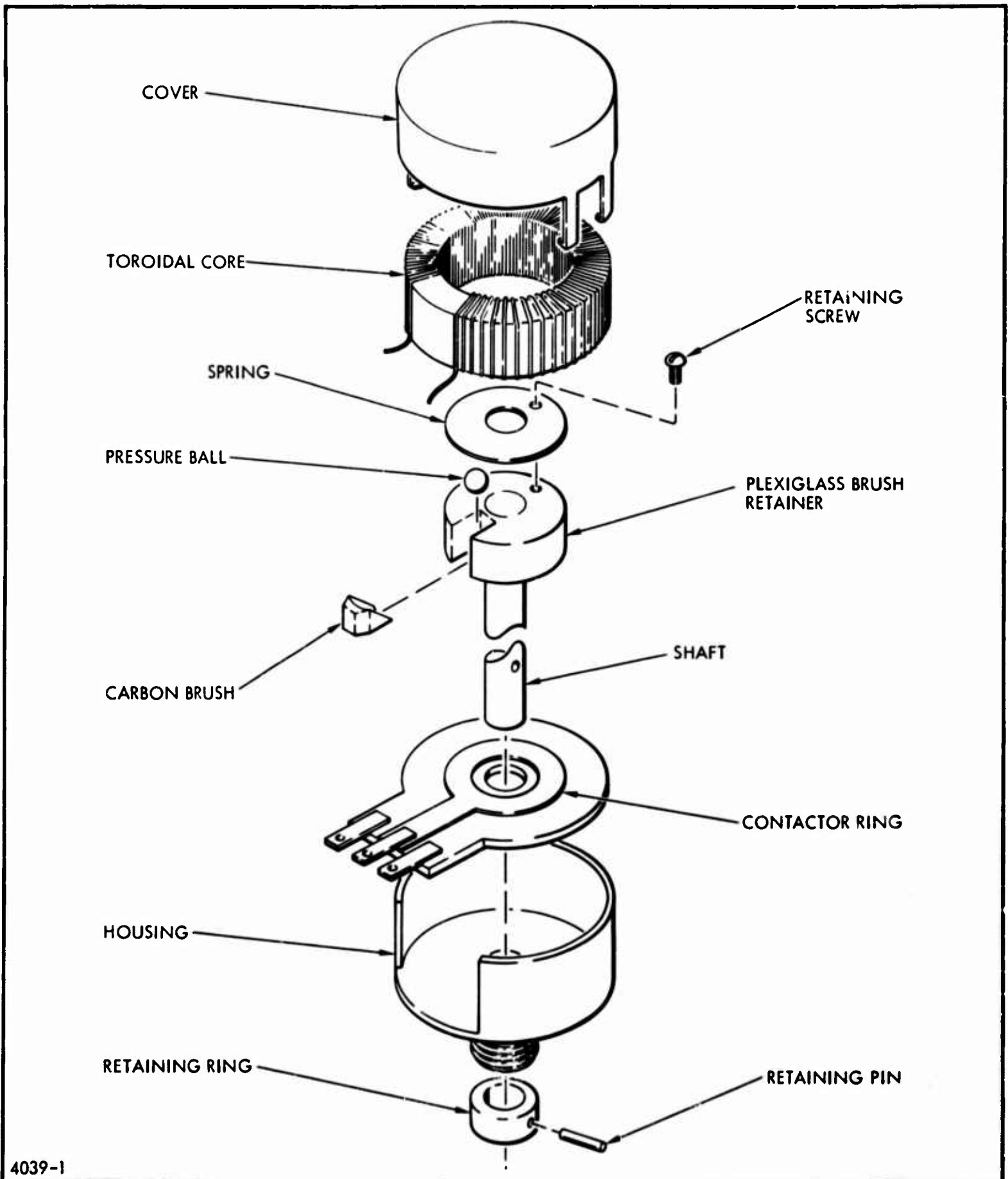


Figure 6 - Construction Details of Variable Transformer

provided for an adjustable tap. A standard Mallary potentiometer is modified to house the core and brush. The resulting device is 0.5 in. in diameter and about 0.5 in. deep, excluding the bushing and shaft.

The high frequency of excitation voltage, 10 kHz, contributes a large measure to the small size of the variable transformer. A lower frequency would require more inductance and, hence, a larger core. A low-loss core material (Supermalloy) and a large number of turns ensure low magnetizing current when excited with 20 v, peak-to-peak, square wave. The carbon brush prevents loss because of shorted turns.

Tests on the prototype of this device have been completed and have been satisfactory in all respects. In operation, the variable transformer will drive a step-up transformer to obtain the required large voltage variations. Tests were made using a 30:1 step-up transformer to obtain a d-c voltage variable from 0 to 300 v. By insulating the step-up transformer secondary, the bridge rectifier may be referenced to a fixed voltage so that variations about a fixed potential is available.

5. VOLTAGE REGULATOR

An input voltage variation of 11.8 to 14.8 vdc will make it necessary to provide regulation for both the cathode-ray tube supply and the integrator-threshold circuits. Preliminary investigation indicated that regulation of the input bus would be more desirable than several individual regulators. A highly efficient regulator was designed and tested to ensure that power loss within the regulator could be reduced to an acceptable level. This circuit at present provides 4-percent regulation and approximately 95-percent efficiency with 20 w into the load. This represents a power loss within the regulator of about 1 w and is relatively constant over the range of input voltage. As a basis of comparison, a standard regulator using a pass transistor to provide an IR drop would consume 3.4 w in the low-voltage case and 8.5 w for the high-voltage condition.

It was recognized at the onset that a duty cycle type regulator would be required to achieve high efficiency. An output voltage of 10 v was chosen, and the design was conducted using a 20-w load. An investigation into the sources of regulator inefficiencies defined circuit configuration and assisted component selection. A compromise was then made between efficiency and weight. A high-frequency chop rate reduces the size and weight of the storage inductor while a low frequency improves efficiency. A chop rate between 5.7 and 7.1 kHz is presently being used and appears near optimum.

Figure 7 is the schematic diagram of the regulator. Q1 and Q3, in conjunction with T1, is basically a magnetic multivibrator. This circuit free runs with Q1 and Q3 alternately going into saturation. For this description, assume Q3 just turning on with the core of T1 saturated in the reverse direction. As Q3 begins to draw current, the three-turn

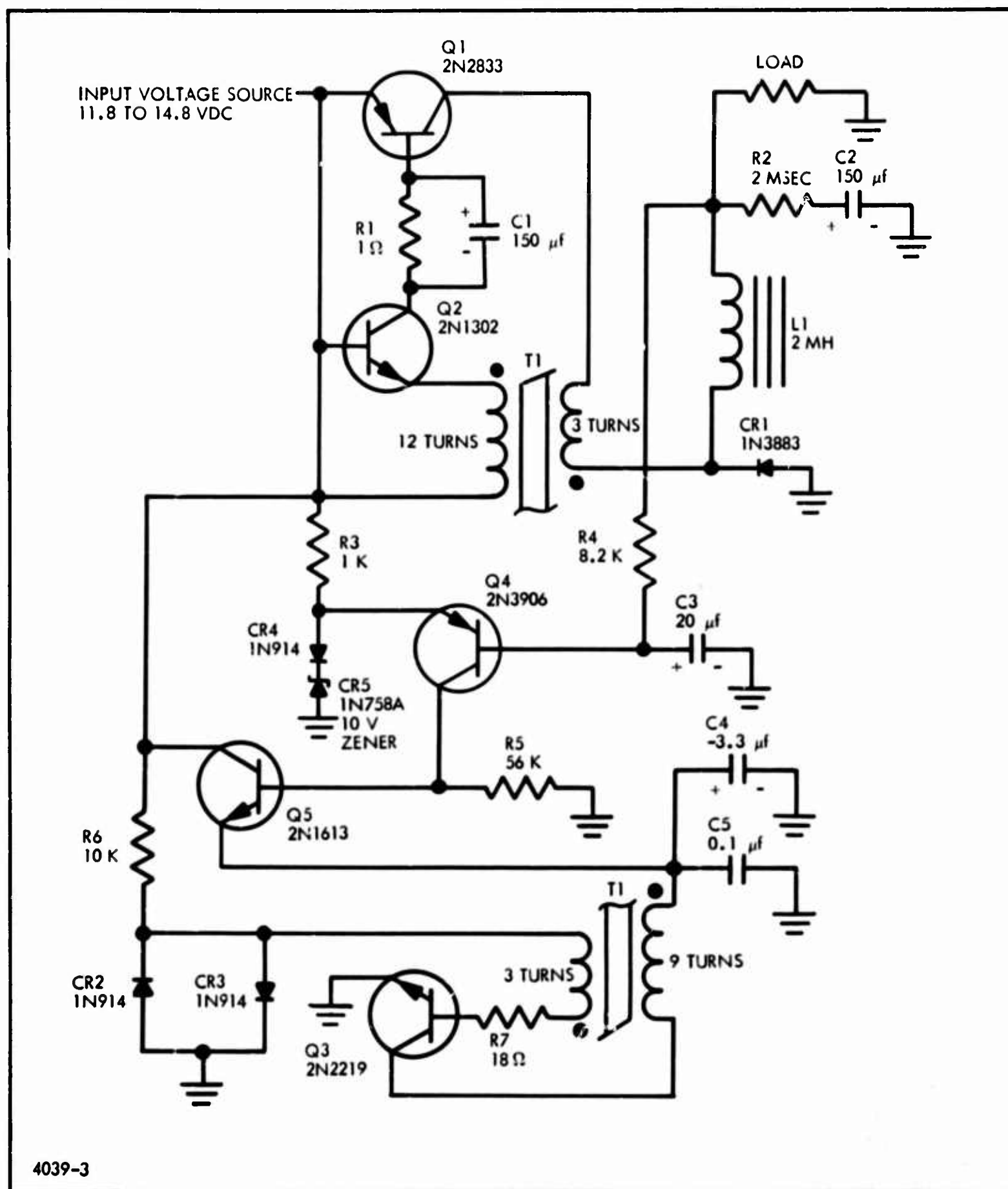


Figure 7 - Voltage Regulator Schematic Diagram

base winding provides Q3 base current through R7 and CR2 and Q3 saturates. Q3 remains saturated until the transformer core saturates in the forward direction. Q3 conduction time, t , is determined by the relationship

$$t = \frac{BNA}{E}$$

where

- B = change in flux density between reverse saturation and forward saturation measured in Tesla (1 Tesla = 1 weber/meter²),
- N = number of turns in collector winding,
- A = core cross section in meters², and
- E = collector supply voltage.

During the time period of Q3 saturation, a positive pulse is presented at the emitter of Q2, and this transistor is cut off. With Q2 cut off, Q1 has no source of base current and it is also cut off. In this condition, no current flows through Q1 into the load. Q2 prevents excessive reverse bias of Q1 emitter base junction while still providing a low-resistance path for Q1 leakage current through the collector-base diode junction of Q2.

When the transformer core reaches saturation in the forward direction, Q3 no longer receives base drive and this transistor cuts off. The flux in T1 now collapses and the emitter of Q2 receives a negative going pulse, causing it to saturate and, in turn, saturate Q1 by providing base current. Q1 would normally remain on until the flux in T1 fell to some small value. However, regeneration is provided by the three-turn collector winding of T1 and Q1 base current flows until T1 saturates in the reverse direction. Q1, however, remains saturated because of the stored charge in the base junction of this transistor. R1 and C1 are included to remove this stored charge and ensure Q1 transition between saturation and cutoff is rapid. The path for the stored charge current is through C1 and the collector base diode junction of Q2. It should be pointed out that this rapid removal of the stored charge is extremely important in obtaining the high efficiency of this circuit.

As Q1 turns off, the collapse of flux in T1 puts a forward bias on the base of Q3 and the cycle is repeated.

From an efficiency point of view, it is well to note that the only power wasted in this circuit is that power consumed by the base circuits of Q1, Q2, and Q3 (plus some power in the regulation amplifier to be described below). The current drawn by Q3 during its conduction cycle is stored in the flux of T1 and provides a large portion of Q1 base drive. Q1 is a germanium device with fast-switching time. Silicon transistors

cannot be used in this application because their large saturation resistance wastes excessive power in the IR drop.

During conduction of Q1, current to the load is supplied through L1. The flux built up in L1 during Q1 conduction, collapses during the off time of Q1 and supplies current to the load through CR1. Capacitor C2 assists L1 in maintaining a constant current through the load. R2 reduces C2 surge current so that L1 does not saturate.

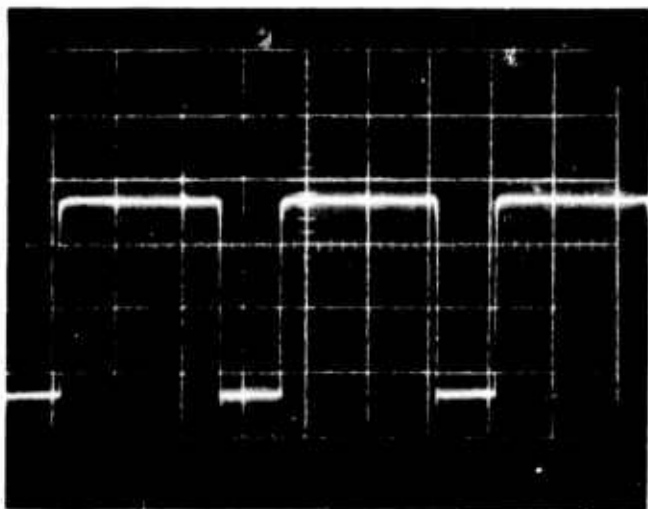
Regulation of output voltage is accomplished by controlling the supply voltage of Q3 and thus its conduction time. Q4 compares the output voltage to a reference voltage across zener diode CR5. CR4 compensates for the emitter base drop of Q4. Power gain is supplied by emitter follower Q5, and C4 and C5 supply the pulse current drawn by Q3. If the output voltage is lower than the reference, Q4 conducts less and Q3 conducts longer because of the lower supply source. Since Q3 conduction time determines the off time of Q1, the output voltage is lowered. It should be noted that the conduction time of Q1 remains constant since Q3 always saturates T1 regardless of its supply voltage.

The efficiency of the regulator is shown in Table II. Figure 8 shows selected waveforms. Note in particular the fast switching time at Q1 collector.

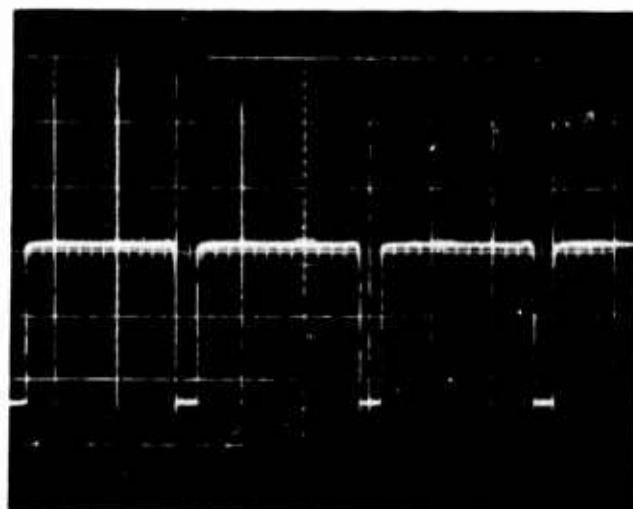
It is not planned to expend further work on this circuit until the final current requirements are obtained. At such time, the circuit will be optimized for the exact operating conditions.

TABLE II - REGULATOR EFFICIENCY

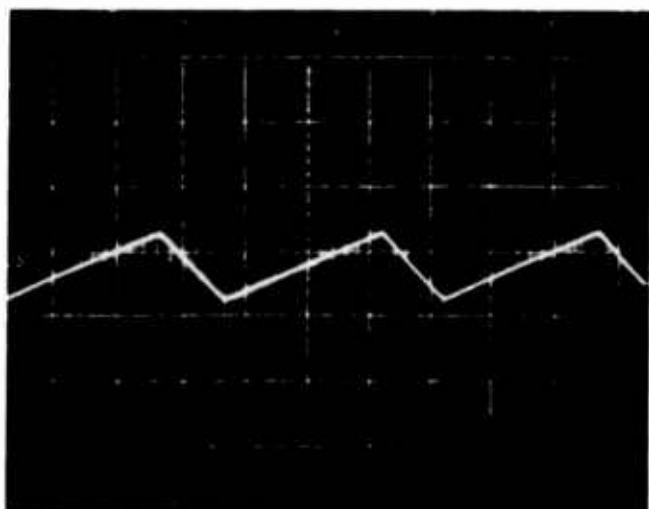
Input voltage	14.8 v	11.8 v
Input current	1.4 amp	1.7 amp
Input power	31.3 w	20.05 w
Output voltage	10.4 v	10.0 v
Output current	1.94 amp	1.90 amp
Output power	20.2 w	20.05 w
Efficiency	94.8 %	94.8 %

**COLLECTOR Q1**

INPUT VOLTAGE = 14.8 VDC
 $V = 5 \text{ V/CM}$, $H = 50 \text{ } \mu\text{SEC/CM}$

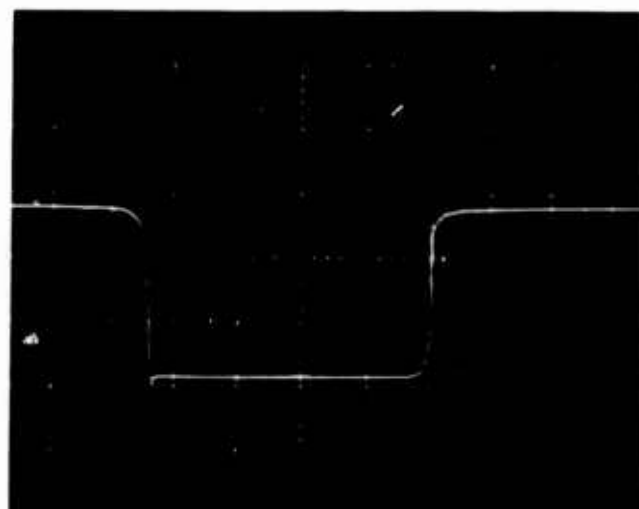
**COLLECTOR Q1**

INPUT VOLTAGE = 11.8 VDC
 $V = 5 \text{ V/CM}$, $H = 50 \text{ } \mu\text{SEC/CM}$

**OUTPUT VOLTAGE RIPPLE**

INPUT VOLTAGE = 14.8 V
 $V = 0.5 \text{ V/CM}$, $H = 50 \text{ } \mu\text{SEC/CM}$

4039-6

**COLLECTOR Q1**

$V = 5 \text{ V/CM}$, $H = 4 \text{ } \mu\text{SEC/10 } \mu\text{SEC}$

Figure 8 - Voltage Regulator Waveforms

6. INTEGRATOR-THRESHOLD CIRCUITS

Pending the outcome of the integrator configuration study, only a limited effort has been expended on the linear integrate and dump circuit. To ensure feasibility of the initial concept, a circuit was breadboarded. This circuit is shown in Figure 9. In the circuit, Q1, Q2, and Q3 form a basic recycle timing generator. The output from Q3 collector turns off Q4 to extinguish the indicator, as described below, and the trailing edge triggers Q3, a blocking oscillator, to generate the threshold strobe signal. The trailing edge of the blocking oscillator pulse triggers the integrator dump generator, Q6 and Q7. The timing relationship is shown in Figure 10. In the schematic diagram, Q9 is a Miller integrator with a time constant determined by C8 and R15. C6, C7, CR5, and CR6 comprise a voltage doubler rectifier to detect the filtered signal. During the time of the integrator dump signal, Q8 saturates and C8 is charged to 10 v through CR8 and the emitter base diode of Q9. CR8 disconnects the collector. Q8 then turns off and the charged capacitor holds Q9 collector at approximately 10 v. If an input signal is present, C8 will be discharged and Q9 collector will integrate toward ground at a rate determined by the time constant and the magnitude of the incoming signal.

Transistors Q10 and Q11 form a regenerative threshold. Q10 is normally conducting and Q11 cut off. When the blocking oscillator fires, a +0.75 v is developed across CR9 and CR10. This voltage is coupled through CR11 to the base of Q11, bringing this base to the conduction point, provided its emitter is at ground. Q11 will thus initiate conduction only during the time interval of the strobe pulse and only if Q9 has integrated to ground potential. If Q11 is allowed this initial conduction, it maintains this condition for a period of approximately 420 μ sec as determined by the feedback connections through Q10 and the time constant of C9 and R20.

The indicator, I1, is a neon connected to +77.5 v through R24 and Q4. The characteristics of this device are such that it will not ionize when Q11 is cut off, since this applies only 67.75 v across the bulb. However, if Q11 is strobed into conduction, full 77.5 v is applied to the bulb and it fires. After the end of the threshold regeneration period, the 67.5 v is sufficient to sustain ionization. The 420- μ sec pulse represents the approximate time of ionization at the potential applied.

Transistor Q4 is provided to extinguish I1 at the beginning of the recycle sequence. With collector of Q3 at ground, Q4 is forward biased through zener diodes CR1 and CR2. When Q4 goes positive, Q4 cuts off, removing the sustaining voltage to I1.

Switches S1 and S2 are provided to alter the normal operation of I1. S1, HOLD, when connected to +10 v, holds Q4 in continuous conduction and I1 will not be extinguished. S2, FREEZE, clamps the bottom of I1 to +10 v and prevents Q11 from ionizing the neon. These two independent controls will provide operational flexibility.

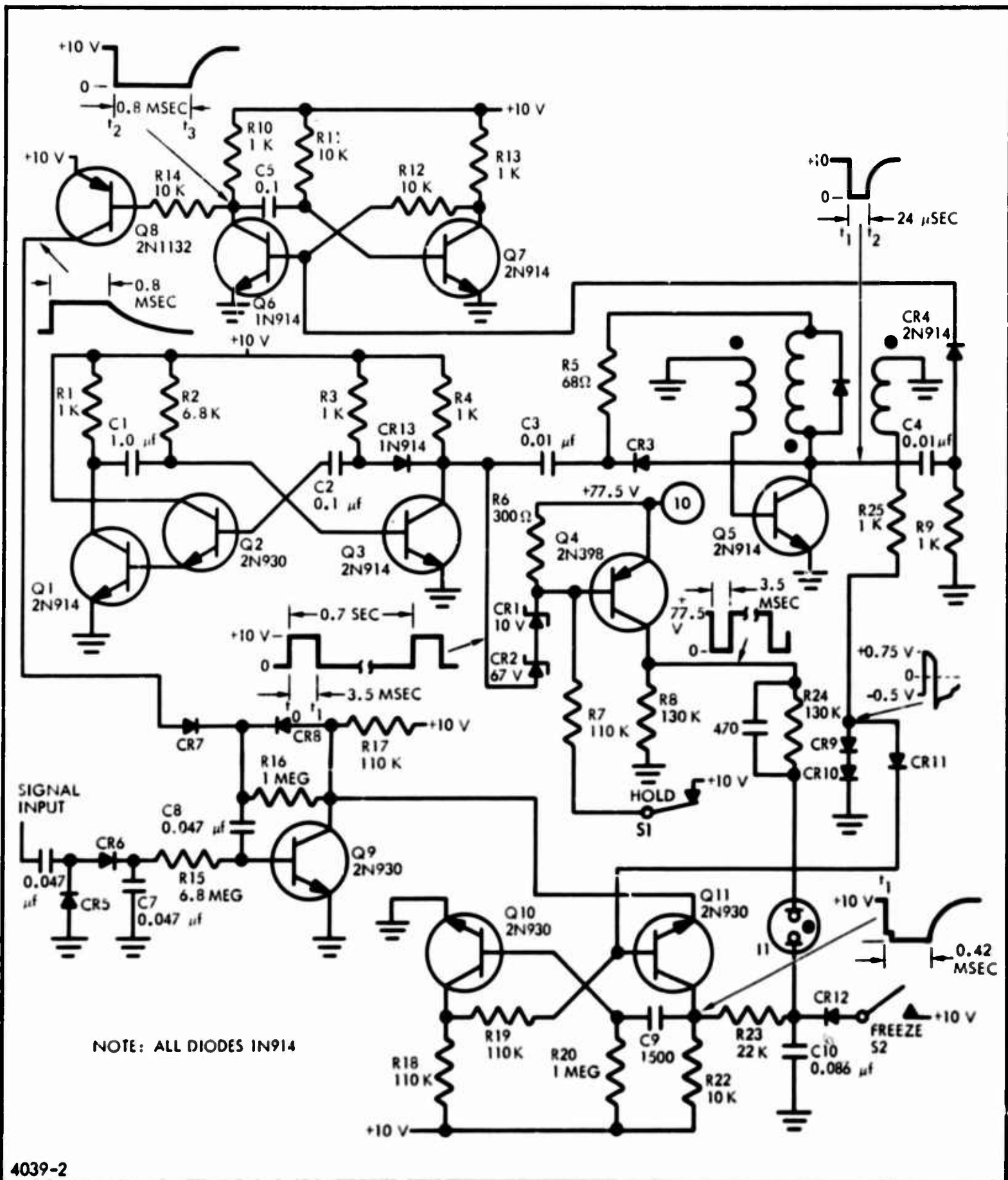
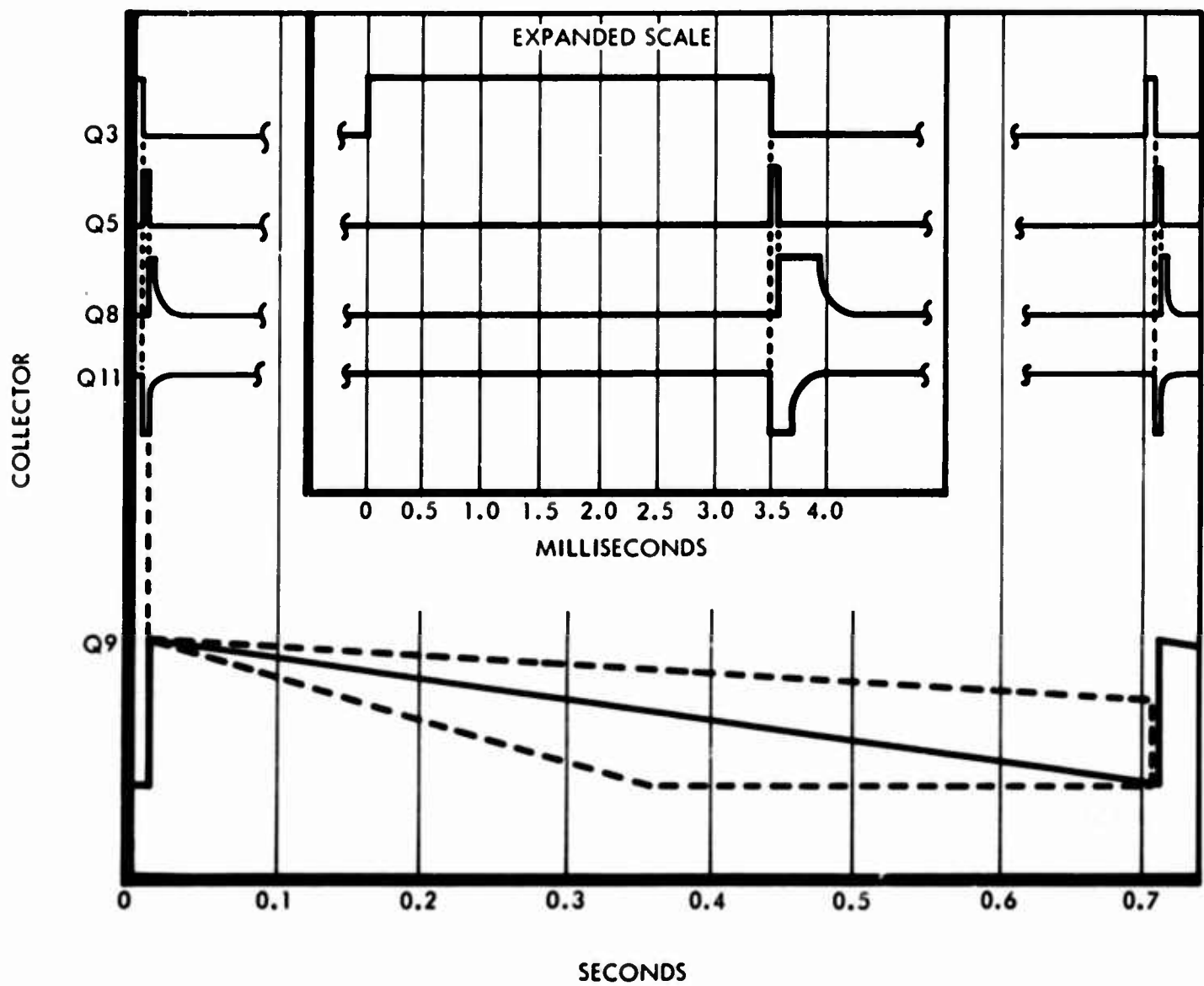


Figure 9 - Integrator-Threshold Test Circuit Schematic Diagram



4039-7

Figure 10 - Integrator-Threshold Circuit Timing Diagram

The integrator, Q9; threshold, Q10 and Q11; and indicator, I1 represent a portion of one individual channel. The remaining circuits will be common to all 100. The power consumption in the integrator and threshold is a maximum of 2 mw, while the indicator consumes 28 mw while conducting. The tests conducted on this circuit have been satisfactory, and a refined version will be utilized in the final design if the integrate and dump technique is chosen.

7. INTEGRATION TECHNIQUE

At the request of the project office, an initial study was undertaken to compare the detection efficiency between a linear-dumped integrator and continuous resistance-capacitance low-pass filter. The study resulted in an algorithm whereby the first probability densities of linear filters can be computed. This work is included at Appendix B. Before the computer programming was undertaken to compute these functions, it was realized that while a comparison between various filter configurations could be made, no insight could be gained as to the optimum filter type.

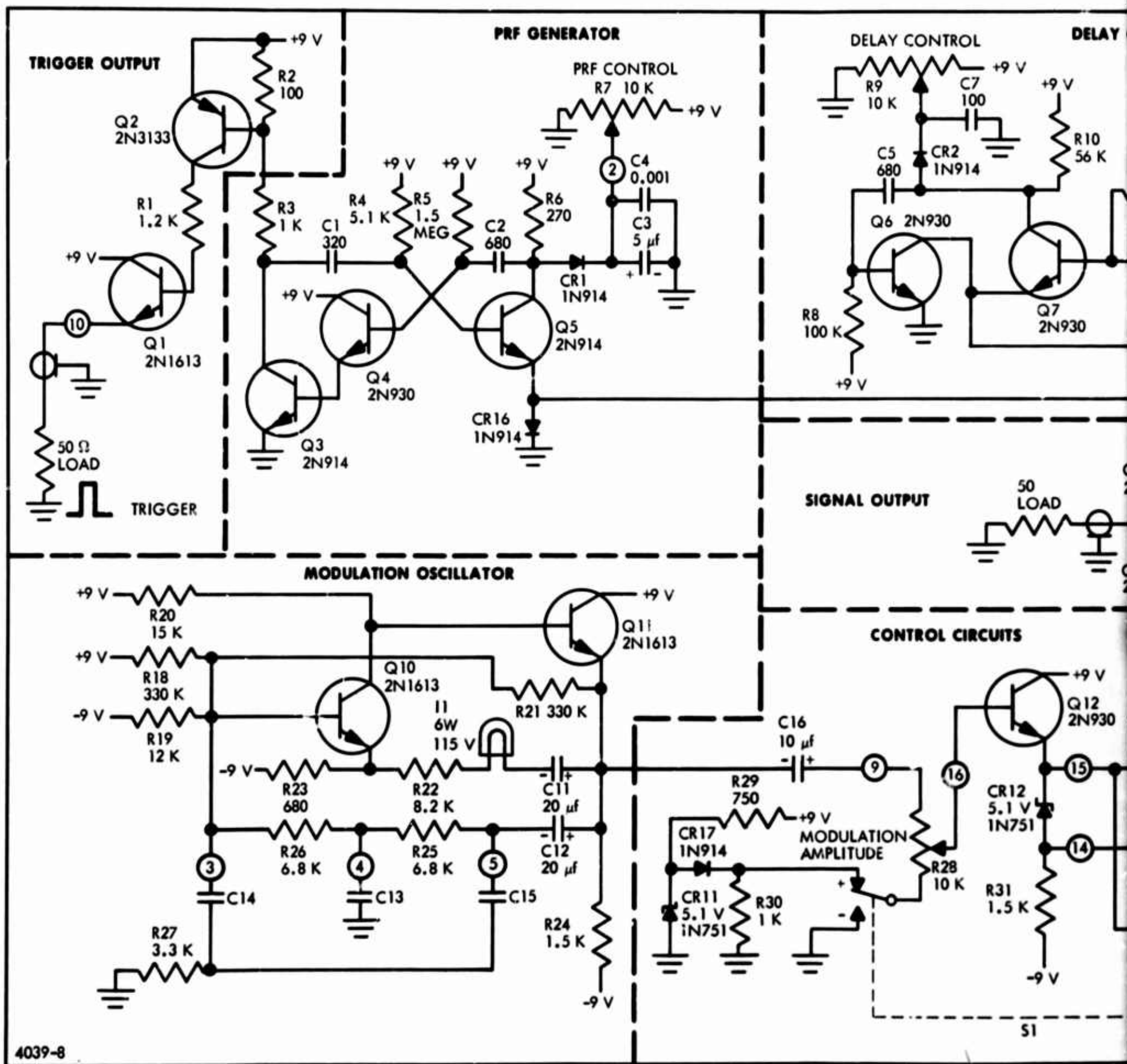
Furthermore, a careful review of the system requirements revealed that even the resistance-capacitance, filter-threshold combination must be periodically sampled since the two indicators require periodic information.

At present, the initial question is still unanswered, but future work will produce far more useful data and allow equipment design to be based on a firm analytical foundation.

8. RADAR SIMULATOR

For testing of the individual range gate channels and the complete system, a radar video simulator is being developed. The target generator and doppler modulator portion has been completed and will be described. The azimuth drive and scan modulator portion is now being designed.

Figure 11 is the schematic diagram of the target generator and doppler modulator portion of the simulator. Q3, Q4, and Q5 comprise a highly unsymmetrical, free-running multivibrator which generates the zero-time trigger at an adjustable pulse rate frequency. Potentiometer, R7, and CR1 clamp the level of Q5 collector when Q5 is cut off and thus control the time duration that Q3 and Q4 are cut off. Since Q5 is cut off for a constant time duration, the cut-off duration of Q3 and Q4 controls the interpulse period and thus the pulse rate frequency. Q2 and Q1 provide power gain to drive a 50-ohm coax with the short positive excursion of Q3 collector.



4039-8

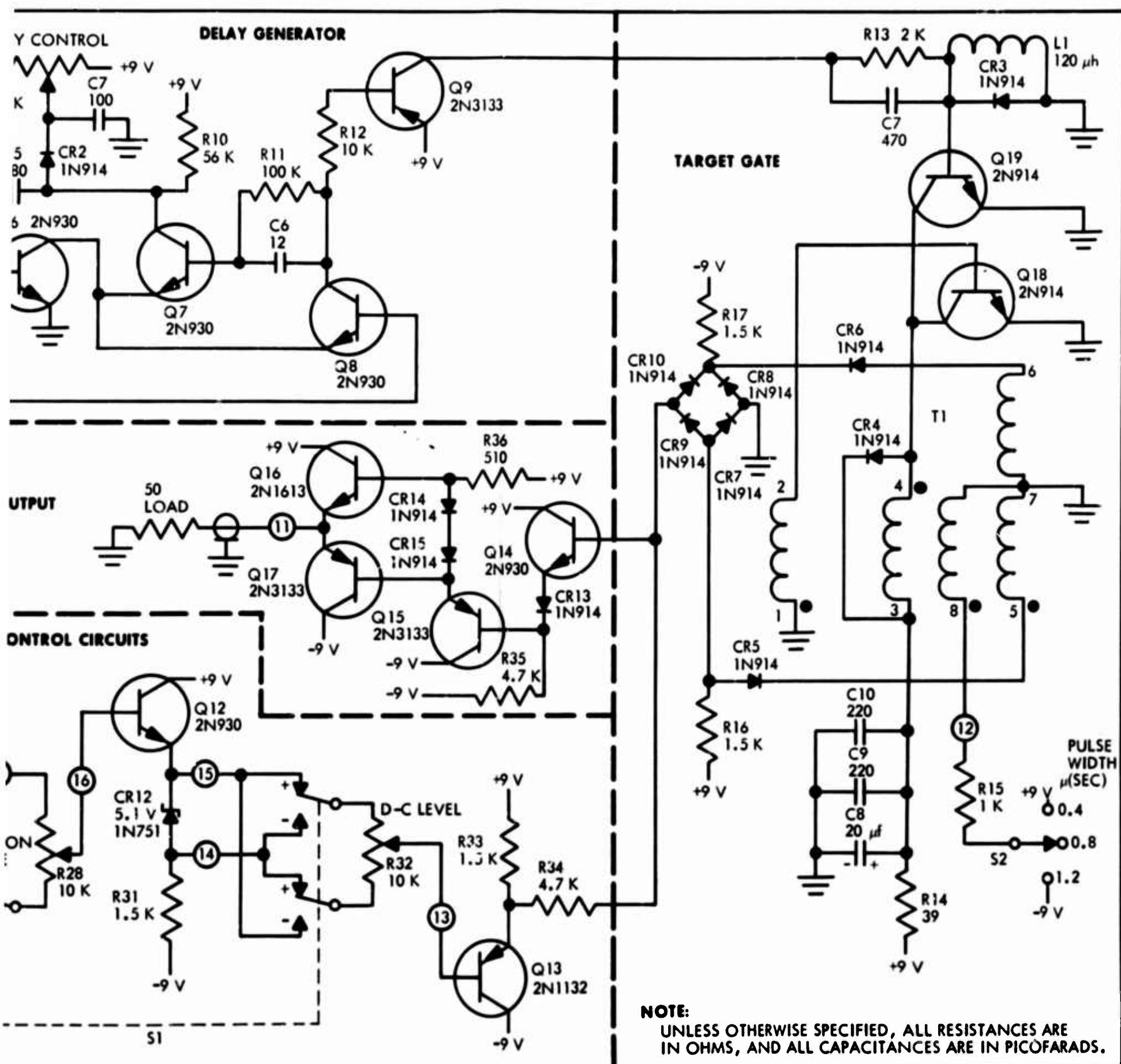


Figure 11 - Target Simulator Schematic Diagram

Transistors Q6, Q7, and Q8 form a self-gated Miller integrator which operates in a manner analogous to the phantastron. This circuit provides a variable delay for the target pulse. The quiescent condition is for Q6 and Q8 saturated and Q7 cut off. Q8 is biased on by the voltage drop across CR16 because of the current through the normally conducting Q5. With Q7 cut off, its collector rises to a level determined by a clamp diode CR2 and potentiometer R9. Thus, a charge is placed across C5. When Q5 cuts off during the generations of the time zero pulse, Q8 cuts off also and its collector rises, turning on Q7. In this condition, Q6, Q7, C5, and R8 form a Miller integrator and collector Q7 runs down toward ground at a linear rate. During the run-down, Q8 is held off since Q6 collector rises above ground. At the end of the run-down, Q6 collector reaches ground and Q8 conducts, turning off Q7 and returning the circuit to its quiescent condition.

The transistorized phantastron circuit provides a linear and stable delay generator. The duration of delay is proportional to the setting of R9 and is insensitive to changes in supply voltage. Jitter is well below the acceptable level.

Q18 and T1 comprise a blocking oscillator circuit which generates the synthetic target. At the termination of the delay circuit, Q9 saturates driving Q19 on for a short time interval. The R-L-C "pipper," R13, C7, and CR3 determine the turn on time of Q19. Q19 parallel triggers the blocking oscillator. The synthetic target width is controlled by a bias winding on transformer T1. Without bias, the blocking oscillator duration is determined by the saturation of T1. Positive or negative bias in the winding, as controlled by S2, either adds or subtracts to the magnetizing current through Q18 and changes the time required for T1 to saturate. Pulses of 0.4, 0.6, or 1.2 μ sec are available.

Simulated doppler frequencies are generated by the modulation oscillator comprised of Q10 and Q11. This is a standard parallel T feed-back oscillator, with positive feed-back through C11, I1, and R22 and negative feedback through C12 and the parallel T network (R25, R26, R27, C13, C14, and C15). Negative feedback exceeds the positive feedback at all frequencies except at the notch frequency of the parallel T, where oscillations can be sustained. I1 acts as a voltage sensitive resistor to stabilize the output amplitude. In the final configuration, C13, C14, C15, and R27 will be switched to allow generation of all 10 of the filter center frequencies. Provision will also be made to allow the use of an external oscillator.

It is necessary to provide a pedestal of variable amplitude and variable modulation level. This is accomplished with the circuits associated with Q11 and Q13. The sine wave from the modulation oscillator is varied in amplitude by potentiometer R28 and referenced at either ground or a plus reference voltage obtained from CR11 and CR12, the d-c level and modulation are coupled into emitter follower C12. Potentiometer R32 across

zener diode CR12 provides an adjustable d-c level shift without changing the modulation level. Thus, R28 controls the amplitude of the sine wave and R32 controls the d-c level, without interaction. Q13 compensates for the emitter-base diode drop of Q12 and provides additional isolation. Switch S1 controls the polarity of the d-c offset.

The simulated target is generated by sampling the sine wave, plus offset, during the pulse period of the blocking oscillator Q18. This is accomplished by a shunt gate (CR5, CR6, CR7, CR8, CR9, and CR10) in conjunction with the series resistor R34. Diodes CR7, CR8, CR9, and CR10 are normally held conducting by the current through R16 and R17, and the junctions of CR9 and CR10 are clamped to ground. When Q18 pulses, CR5 and CR6 conducts back biasing the diode bridge. During this time interval, the signal at the emitter of Q13 is passed through R34 to the base of Q14. The shunt-type gate was chosen because it is low impedance and thus insensitive to stray pickup. The six-diode gate configuration does not require balancing of the diodes and driver pulses.

Q14, Q15, Q16, and Q17 provide sufficient power gain to drive a 50-ohm load with a 5-v, peak-to-peak, signal. All transistors are operated as emitter followers and thus the voltage gain is unity. The complimentary emitter followers, Q16 and Q17, ensure good transition in both the positive and negative directions. CR14 and CR15 prevent crossover distortion in the output transistors, and CR13 compensates for Q15 emitter-base drop. This circuit is capable of driving a 50-ohm load at a level of either ± 5 v.

Figure 12 shows the waveform of the target output with five different set up conditions. Also shown is the zero-time trigger pulse.

SECTION IV - CONCLUSIONS

The work accomplished during this reporting period has proven the feasibility of many of the original concepts. The most noteworthy accomplishments are:

1. Determination of the S-plane parameters for all 10 filters and synthesis of 1 filter using integrated-circuit d-c amplifiers rather than inductors.
2. Design of a 20-w input voltage regulator with an efficiency of 95 percent.
3. Demonstration of techniques to realize a highly efficient, high-voltage power supply.
4. Design of an extremely small variable transformer.
5. Fabrication of the video portion of a radar target simulator.

LIST OF REFERENCES

1. Guillemin, E. A.: Synthesis of Passive Networks. New York, J. Wiley & Sons, 1957; Chapter 14.
2. Weinberg, L.: Network Analysis and Synthesis. New York, McGraw-Hill, 1962; pp 514-517.
3. Todd, Carl D.: A Versatile Negative Impedance Converter. Semiconductor Products; May 1963, pp 25-29; and June 1963, pp 27-33.
4. Klein, G. and Zaalberg van Zelst, J. J.: Some Simple Active Filters for Low-Frequency. Phillips Technical Review, 1963/64; Volume 25, pp 330-340.
5. Gile, William: Solid-State, Low-Frequency Filter. Electro-Technology, September 1964; pp 34-37.
6. Beauchamp, K. G.: Active Filter Design. Engineering Design News, August 1964.
7. Strunk, B.: Designing an Active Filter. Electronic Equipment Engineering, October 1965.

APPENDIX A - HUMAN FACTOR ENGINEERING SELECTION CRITERIA FOR AZIMUTH-RANGE DISPLAY

The following criteria should be considered in selection of a crt for ADDEM azimuth-range display:

1. Azimuth-Range Display Signal Size

It is recommended that 18 in. viewing distance be used by operator for observing azimuth-range display, with 16 in. as the minimum normal viewing distance which can be used without fatigue. A minimum signal size of 5.3×10^{-3} in. is required for high-probability detection at an 18 in. viewing distance. Presently anticipated azimuth-range display signal dimensions of 0.045 in. length by 0.011 in. width fall well within these limits.

2. Screen Brightness

The operator in the field may visually adapt to higher brightness levels than that of the shielded display area because of either his performing other visual tasks or to boredom in fixating only on the display face. To ensure visibility of the azimuth-range display signals under most field conditions (including a clear or hazy day in the desert, snow on the ground, etc.), a scope brightness of 100 mL is required. A minimum scope brightness of 20 mL will suffice for signal visibility under average conditions.

3. Signal Duration

A minimum signal duration time of 0.2 sec is required for high-probability detection.

4. Signal-Background Contrast

To ensure high-probability detection of azimuth-range display signals: an 8-percent contrast is required for a 100-ft.-L background, and a 10-percent contrast is required for a 50-ft.-L background.

$$\text{Percent Contrast} = \frac{B_1 - B_2}{B_1} \times 100,$$

where

B_1 = signal brightness

B_2 = background brightness.

APPENDIX B - AN ALGORITHM FOR THE COMPUTATION OF FIRST PROBABILITY DENSITIES AT THE OUTPUT OF A LINEAR FILTER FOR A NON-GAUSSIAN INPUT^a

The purpose of this appendix is to enable one to evaluate the effect of post detection filtering on the signal detection properties of radar receivers. No attempt has been made to derive or justify the equations given here and only the key equations necessary for evaluating the system are shown. For a detailed description of the mathematical technique, the reader is referred to the references.

The probability density function at the output of the video filter, for noise alone and for signal plus noise, will be the basic element for the evaluation of the system. It is assumed that the usual threshold detector follows the video filter. The false alarm probability is defined as the probability that the output of the video filter (no signal present) exceeds the threshold voltage. The detection probability is similarly defined as the probability that the output of the video filter (both signal and noise present) exceeds the threshold. These two probabilities are illustrated in Figure B1. With this information, a comparison of different video filters may be made by setting the detection probabilities equal and observing the false alarm probabilities for the several filters. Of course, the threshold voltages are not necessarily the same for the various filters.

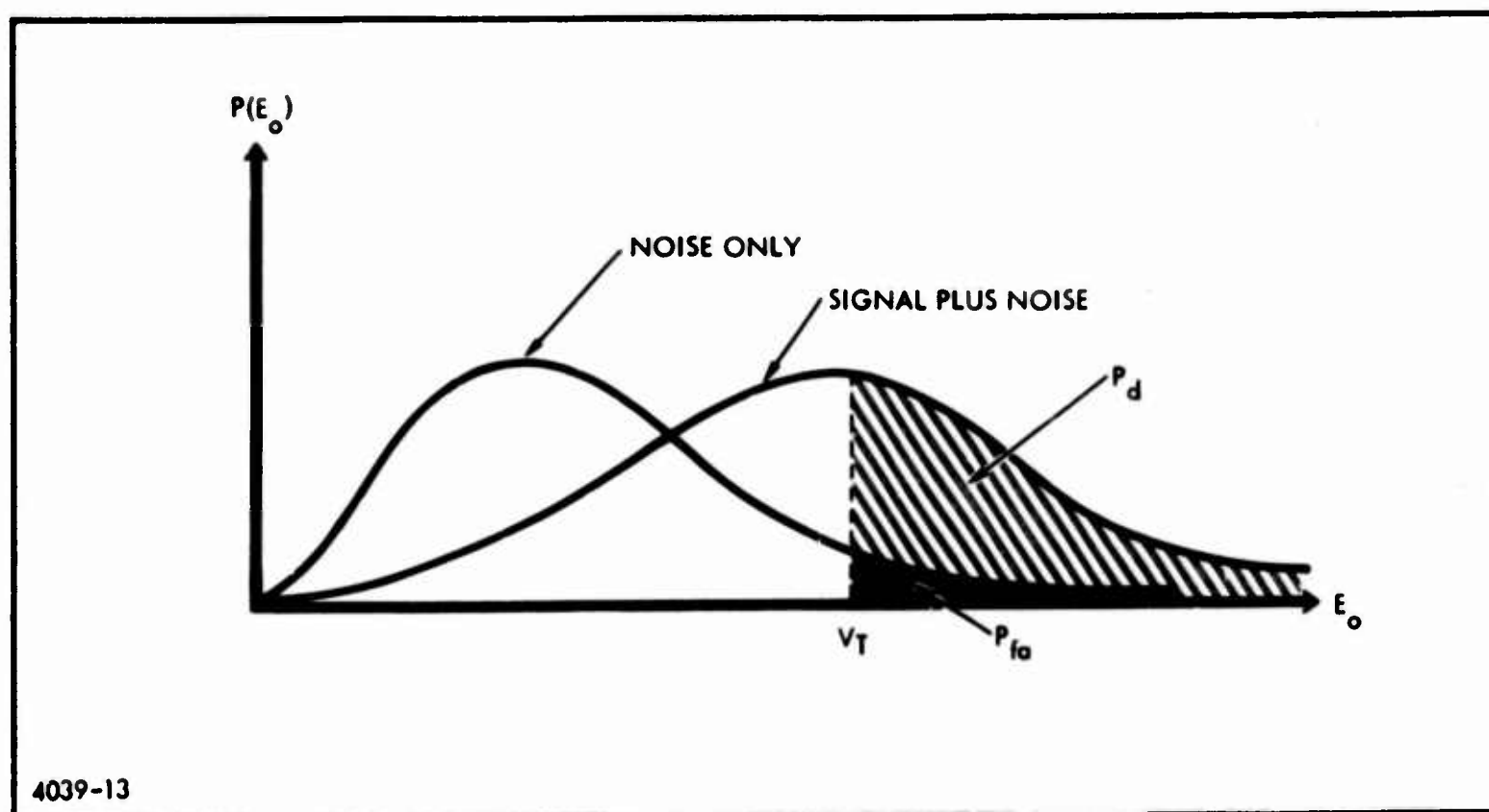


Figure B-1- Detection Probabilities for Noise Only and Signal Plus Noise

^a For List of Symbols, see page 39.

The system is shown in Figure 2.



Figure B-2- Basic System

With the density of $E_o(t)$, the false alarm probabilities for different video filters (same detection probability) may be obtained.

Let the input be $E_i(t) = S(t) + N(t)$ where $N(t)$ is white gaussian noise and $S(t) = a(t) \cos \omega_0 t$; $a(t)$ is low-frequency modulation.

Two different video filters are considered - one filter is $h_2'(t)$ and the other filter is $h_2''(t)$. The calculation of the detection probability implies (by definition) the use of the density function for signal plus noise, and the false alarm probability is never calculated with a signal present (also by definition).

Let the probability density function for the output voltage be $P_1(E_o)$ when $h_2'(t)$ is used and $P_2(E_o)$ when h_2'' is used. Assuming identical inputs (signal and noise amplitudes) for the two cases, the detection probability is given by

$$\int_{V_{T_1}}^{\infty} P_1(E_o) dE_o = \int_{V_{T_2}}^{\infty} P_2(E_o) dE_o = P_d \quad (B-1)$$

Now that the threshold voltages V_{T_1} and V_{T_2} have been determined for a fixed detection probability, the false alarm probability may be computed from the density function for noise alone.

$$P_{fa_1} = \int_{V_{T_1}}^{\infty} P_1(E_o) dE_o \quad (B-2)$$

$$P_{fa_2} = \int_{V_{T_2}}^{\infty} P_2(E_o) dE_o$$

With this information, a comparison of the two systems can be made.

Except in certain cases (e.g., infinitely wide video bandwidth, in which case the curves of Marcum and Swerling^a may be used) where it is possible to determine the eigenvalues of various integral equations, it is not generally possible to write an exact expression for $P(E_o)$ in closed form.

$$P(E_o) = \frac{1}{\sqrt{K_2}} \sum_{j=0}^{\infty} \alpha_j \phi^{(j)} \left(\frac{E_o - K_1}{\sqrt{K_2}} \right) \quad (B-3)$$

where

$$\phi^{(j)}(x) = \frac{d^j}{dx^j} \left\{ \frac{1}{\sqrt{2\pi}} e^{-x^2/2} \right\}.$$

Here, the α_j 's depend only on K_n , and the K_n 's are the cumulants.

An algorithm will now be described for computation of the cumulants so that the density may be determined. This is based on the theory presented by Emerson.^b

Using the convolution operation, the output may be expressed in terms of the input, $E_i(t)$, and the system kernel $g(u, v)$:

$$E_o(t) = \int_{-\infty}^{\infty} \int_{-\infty}^{\infty} E_i(t-u) g(u, v) E_i(t-v) du dv \quad (B-4)$$

where

$$g(u, v) = \int_{-\infty}^{\infty} h_1(u-z) h_2(z) h_1(v-z) dz.$$

The limits of integration have been extended over the entire real axis, but, in a fixed, physical, linear system, the functions h_1 and h_2 will vanish for negative arguments.

^a Marcum, J. I.; and Swerling, P: A Statistical Theory of Target Detection by Pulsed Radar with Mathematical Appendix. Rand Corporation, Reports RM-753 and RM-754.

^b Emerson, R. C.: First Probability Densities for Receivers with Square Law Detectors. Journal of applied Physics, Volume 24, Number 9, pp 1168-1176.

The characteristic function for the square law detector has been given by Emerson and Davenport and Root^a as

$$\Phi(\xi, t) = \prod_{i=1}^{\infty} \left| 1 - 2j\xi\lambda_i N_0 \right|^{-1/2} \times \exp \left[\frac{s_j(t)^2}{2N_0} \frac{2j\xi\lambda_i N_0}{1 - 2j\xi\lambda_i N_0} \right] \quad (B-5)$$

where N_0 is the noise power spectral density and the λ_i 's are the eigenvalues of the integral equation

$$\lambda h(x) = \int_{-\infty}^{\infty} g(x, y) h(y) dy \quad (B-6)$$

Let $\{h_j\}$ be the set of orthonormal eigenfunctions corresponding to the set $\{\lambda_j\}$; then $s_j(t)$ is defined as

$$s_j(t) = \int_{-\infty}^{\infty} S(t-x) h_j(x) dx \quad (B-7)$$

The cumulants may be found by expanding $\ln\Phi(\xi)$ in powers of $j\xi$.

$$\sum_{n=1}^{\infty} K_n \frac{(j\xi)^n}{n!} = \ln\Phi(\xi) \quad (B-8)$$

The formula for the n^{th} cumulant is

$$K_n(t) = (2N_0)^n \frac{n!}{2} \left\{ \frac{1}{n} \int_{-\infty}^{\infty} g^n(u, u) du + \frac{1}{N_0} \int_{-\infty}^{\infty} \int_{-\infty}^{\infty} S(t-u) g^n(u, v) S(t-v) dudv \right\} \quad (B-9)$$

^aDavenport, W. B.; and Root, W. L.: An Introduction to the Theory of Random Signals and Noise. New York, McGraw-Hill Book Co., Inc., 1958.

where

$$g^n(u, v) = \int_{-\infty}^{\infty} \int_{-\infty}^{\infty} g(u, x_1) g(x_1, x_2) \times g(x_{n-1}, v) dx_1 \dots dx_{n-1}.$$

When the video bandwidth is small compared to the i-f bandwidth, $P(E_0)$ is near'y gaussian; let the density function be expanded in a Gram-Charlier series:

$$P(E_0) = \frac{1}{\sqrt{K_2}} \sum_{j=0}^{\infty} \alpha_j \phi^{(j)} \left(\frac{E_0 - K_1}{\sqrt{K_2}} \right) \quad (B-10)$$

where

$$\phi^{(j)}(x) = \frac{d^j}{dx^j} \left\{ \frac{1}{\sqrt{K_2}} \exp \left(-\frac{x^2}{2} \right) \right\}$$

and

$$\alpha_0 = 1$$

$$\alpha_1 = \alpha_2 = 0$$

$$\alpha_3 = -\frac{K_3}{6K_2^{3/2}}.$$

To recapitulate, given the filter transfer functions, compute $g(u, v)$ and $g^n(u, v)$. Then compute the cumulants K_1 , K_2 , and K_3 and sum the above series to obtain $P(E_0)$.

Emerson has presented normalized curves for $P(E_0)$, assuming the input signal is $S(t) = \sqrt{2S} \cos \omega_0 t$ and the i-f and video filters have a gaussian passband, for several values of bandwidth ratio and three values of signal-to-noise ratio. Davenport and Root give a solution when $h_2(t)$ is an integrator and $h_1(t)$ is resistance capacitance low pass (shifted up in frequency), for noise only at the input, in terms of the solution of a well-known integral equation.

LIST OF SYMBOLS

α_j = coefficients in the expansion of the output probability density function

ξ = dummy variable in the characteristic function

λ_1 = orthonormal eigenvalues of an integral equation

$\phi^{(j)}(x)$ = orthogonal functions in the expansion of the output probability density function

$\Phi(\xi, t)$ = the characteristic function of the output probability density

$a(t)$ = low-frequency modulation at the input

$E(t)$ = output of the bandpass filter

$E_i(t)$ = input to the bandpass filter

$E_o(t)$ = output of the video filter

$g(u, v)$ = the system kernel, defined on page 36.

$h_1(t)$ = impulse response of the bandpass filter

$h_2(t)$ = impulse response of the video filter

$h_2'(t), h_2''(t)$ = two different video filters

$h_j(x)$ = the orthonormal eigenfunctions corresponding to the eigenvalues λ_j

$K_n(t)$ = the cumulants of the output probability density function

$N(t)$ = white gaussian noise at the input

N_o = power spectral density (double sided) of the input noise.

P_d = detection probability

P_{fa} = false alarm probability

$P(E_o)$ = probability density function at the output of the video filter

$S(t)$ = input signal

$s_j(t)$ = coefficients in the expansion of $S(t)$ in terms of $h_j(x)$

V_T = threshold voltage of the threshold detector following the video filter

APPENDIX C - DERIVATION OF ACTIVE FILTER TRANSFER FUNCTION

The transfer functions given in Equation (7) for the active filter of Figure 3(A) are derived from the generalized configuration shown in Figure C-1.

In this circuit,

$$E_{1N} = \frac{1}{Y_1} I_1 + E_1 . \quad (C-1)$$

Replacing I_1 with $I_1 = I_2 + I_3 + I_4$ gives

$$E_{1N} = \frac{1}{Y_1} (I_2 + I_3 + I_4) + E_1 . \quad (C-2)$$

Because of the virtual ground and high input impedance at the amplifier input, the following approximations can be made:

$$E_{Y_2} = E_{Y_3} = E_1$$

and

$$I_3 = I_5 .$$

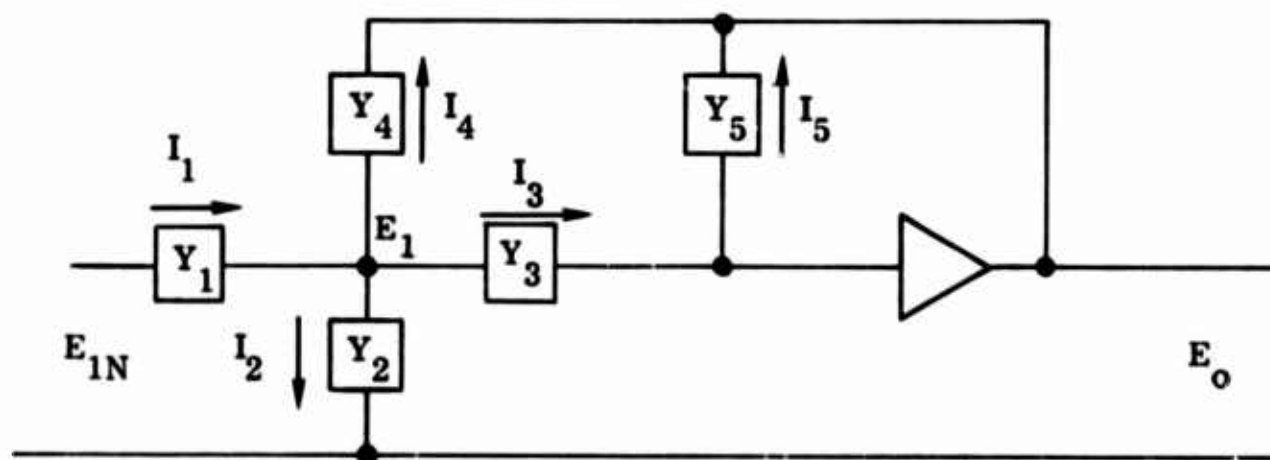


Figure C-1 - Generalized Configuration

Also,

$$E_{Y_4} = E_1 - E_o.$$

Currents I_2 , I_3 , and I_4 can then be expressed as:

$$I_2 = Y_2 E_{Y_2} = Y_2 E_1 \quad (C-3)$$

$$I_3 = Y_3 E_{Y_3} = Y_3 E_1 \quad (C-4)$$

$$I_4 = Y_4 E_{Y_4} = Y_4 (E_1 - E_o). \quad (C-5)$$

Substituting these into Equation (C-2) gives

$$E_{1N} = \frac{1}{Y_1} \left[Y_2 E_1 + Y_3 E_1 + Y_4 (E_1 - E_o) \right] + E_1. \quad (C-6)$$

E_1 is obtained by equating I_3 and I_5 as

$$I_3 = Y_3 E_1 = -Y_5 E_o = I_5 \quad (C-7)$$

to give

$$E_1 = \frac{-Y_5 E_o}{Y_3}. \quad (C-8)$$

Replacing E_1 in Equation (C-6) results in

$$\begin{aligned}
 E_{1N} &= \frac{1}{Y_1} \left[Y_2 \left(\frac{-Y_5}{Y_3} \right) E_o + Y_3 \left(\frac{-Y_5}{Y_3} \right) E_o + Y_4 \left(\frac{-Y_5}{Y_3} - 1 \right) E_o \right] - \frac{Y_5}{Y_3} E_o \\
 &= \frac{E_o}{Y_1} \left[-\frac{Y_2 Y_5}{Y_3} - \frac{Y_3 Y_5}{Y_3} - \frac{Y_4 Y_5}{Y_3} - \frac{Y_4 Y_3}{Y_3} - \frac{Y_5 Y_1}{Y_3} \right] \\
 &= \frac{E_o}{Y_1 Y_3} \left[-Y_2 Y_5 - Y_3 Y_5 - Y_4 Y_5 - Y_4 Y_3 - Y_5 Y_1 \right] \quad (C-9)
 \end{aligned}$$

Collecting terms and rearranging results in the generalized transfer function

$$\frac{E_o}{E_{1N}} = \frac{-Y_1 Y_3}{Y_5 (Y_1 + Y_2 + Y_3 + Y_4) + Y_4 Y_3} \quad (C-10)$$

For the specific case shown in Figure 3(A),

$$Y_1 = s C_2$$

$$Y_2 = 0$$

$$Y_3 = \frac{1}{R_2}$$

$$Y_4 = \frac{1}{R_1}$$

$$Y_5 = s C_1$$

From Equation (C-10), the specific transfer function is derived as:

$$\begin{aligned}
 \frac{E_o}{E_{1N}} &= \frac{-\frac{S C_2}{R_2}}{S C_1 \left(S C_2 + \frac{1}{R_2} + \frac{1}{R_1} \right) + \frac{1}{R_1 R_2}} \\
 &= \frac{-\frac{S C_2}{R_2}}{S^2 C_1 C_2 + \frac{S C_1}{R_2} + \frac{S C_1}{R_1} + \frac{1}{R_1 + R_2}} \\
 &= \frac{-S C_2 R_1}{S^2 C_1 C_2 R_1 R_2 + S C_1 R_1 + S C_1 R_2 + 1} \quad (C-11)
 \end{aligned}$$

SUPPLEMENT TO REPORT NO. 1; DATED 9 NOVEMBER 1965 THROUGH 31 JANUARY 1966,
FOR SERVICES UNDER CONTRACT NO: DA-28-043 AMC-0711(E)

1. IDENTIFICATION OF KEY TECHNICAL PERSONNEL

The following is a list of key technical personnel and the manhours performed by each on the Automatic Detection and Display Equipment for the moving-target indicator program from 9 November 1965 through 31 January 1966.

Name	Title	Manhours
Ford, R. A.	Development Engineer	112
Knight, C. C.	Design Engineer	79
Miller, C. R.	Development Engineer	391
O'Herren, D. H.	Development Engineer	211
Schoenfeld, L. L.	Project Engineer	313
Wood, B. C.	Development Engineer	173

Below is a brief résumé of key personnel who are assigned direct work on the proposed project.

SCHOENFELD, L. L.

Education: U. S. Army Radar Technical Schools

Experience: Mr. Schoenfeld spent 7 1/2 years in the U. S. Army as a radar repairman and was discharged in 1954 with the rank of MSgt. His service experience includes 4 years with the White Sands Signal Corps Agency at Holloman Air Force Base, New Mexico, and White Sands Proving Ground, New Mexico, where he was primarily associated with tracking radars and data handling equipment. During 1953 and 1954, Mr. Schoenfeld was assigned to the 8th Army Signal Corps Depot, Yong Dang Po, Korea, as Noncommissioned Officer in Charge of the Radar Repair Section. During this assignment, Mr. Schoenfeld contributed to the introduction of the AN/MPQ-10 Counter Mortar Radar to the Korean theater. In addition to repair, maintenance, and alignment of this radar, he conducted on-site visits to the operational sites and developed a modification to the sector scan circuit that prevented azimuth drive motor burnout.

Upon joining Goodyear Aerospace, Mr. Schoenfeld took part in the flight testing of the MACE missile. Since 1956, he has worked with system and

circuit design for digital data transmission techniques. He was project engineer for the Goodyear Aerospace miniaturized teletypewriter and contributed to the design and testing of synchronizers, motion compensating circuits, and recorders for synthetic aperture radars. Later, he was in charge of the Field Service modification-retrofit and training section for the AN/APQ-102 program. At present, Mr. Schoenfeld is conducting studies for advanced systems and techniques for the Research and Development Section.

FORD, ROBERT A.

Education: BS, Electrical Engineering, Columbia University, New York, New York, June 1964
MS, Electrical Engineering, Columbia University, New York, New York, June 1965

Experience: During the summer of 1963, Mr. Ford worked at the Microwave Laboratory, Columbia University, on the propagation of slow electromagnetic waves on a plasma column. The following summer he was employed at the Electronics Research Laboratories, New York City, where he performed system studies for Nike-X and investigated detection probabilities for phased array radars.

Since June 1965, Mr. Ford has been employed with Goodyear Aerospace on phase coding techniques for digital chirp and distributed parameter pulse compression filters. He is currently examining the noise properties of receivers with post-detection filtering.

O'HERREN, DAVID H.

Education: BS, Chemical Engineering, Purdue, Lafayette, Indiana, 1950
Electrical Engineering, Arizona State University, Tempe, Arizona, Masters Program, 1961 to 1963

Experience: Mr. O'Herren worked from 1950 to 1961 as a process engineer for Radio Corporation of America's Record Department. High fidelity sound reproduction was the central area of work interest.

He joined the Electronics Engineering Department of Goodyear Aerospace in 1963, being associated since then with the Digital Computer Applications Group. Areas of specialization include:

1. Optical systems design packages
2. Fourier analysis
3. Electronic circuit analysis
4. Digital computer programming systems.

In 1965, Mr. O'Herren converted the Automatic Lens Correction program, written for the large scale IBM 7090 digital computer, for use on the small scientific IBM 1620 computer of Goodyear Aerospace. He also completed a generalized electronic circuit analysis programming system.

KNIGHT, C. C.

Education: Diploma in Aeronautical Engineering, Cal-Aero Technical Institute

Experience: For 6 years, Mr. Knight was employed by Melpar, Inc., Falls Church, Virginia, as a draftsman and then as a senior draftsman. He was engaged in the electromechanical design of printed circuit boards, rack mounting equipment, telemetering beacons, and airborne electronic boxes.

Mr. Knight joined Goodyear Aerospace in January 1956, as a senior design engineer. His duties have included the electromechanical design of optical transducers for the Artemis program and the electromechanical design for an electronic tape printer and keyboard. For the 665A program, he participated in the mechanical design, assembly, and checkout of the electro-mechanical, optical, and film processing of the in-flight correlator-processor. On the RF-4C program, he has checked out the electromechanical, optical, and film processing components of the correlator and has done redesign work for it.

MILLER, C. R.

Education: ICS Radio
USAF Fighter Command VHF School

Experience: Mr. Miller's radio service and engineering experience date from 1929 through 1941, after which he served as a communications officer (overseas) for 30 months. Upon completion of his service, he joined KOY as chief engineer for their radio and TV stations. Mr. Miller joined Goodyear Aerospace as a development engineer in 1955 and was responsible for the development of the synchronizer for the TRITON missile and the SSCM programs. Later, he worked on the i-f modulator, synchronizer, demodulator, offset generator, and motion compensation for the AN/APS-73(XH-2) and Quick-Check radar system.

WOOD, B. G.

Education: BS, Education, Eastern Illinois University
AB, Physics, University of California, Berkeley, California
MS, Electrical Engineering, University of Arizona, Tempe, Arizona
Graduate Studies, Syracuse University, Syracuse, New York, and Arizona
State University. Voluntary Education Courses, IBM, Endicott, New York.

Experience: Upon graduation from the University of California in 1956, Mr. Wood joined Goodyear Aerospace and worked on such projects as a mechanical scanner and mapmaking device, programming an analog computer for the optimum filtering of doppler radar data, and timing circuitry for the radar data processor for the B-70 program.

In 1960, Mr. Wood left Goodyear Aerospace to work for International Business Machines Corporation, General Products Division, Endicott, New York, in the Bank Systems area. While there, he built a magnetic character-sensing and recognition system and supervised the electrical work on a check-endorsing device for the IBM high-speed electronic sorter. Several patent applications are on file as a result of his work in these areas. In addition to his full-time work, Mr. Wood was an instructor in the IBM evening voluntary education program and taught several mathematics and solid-state physics courses.

In 1963, Mr. Wood returned to Goodyear Aerospace and is presently project engineer on a company-funded project to produce an all-electronic doppler radar processor. This device involves a scan-converter storage tube and a video tape recorder of unique design.

2. CONFERENCES

The following conferences were held during the reporting period.

Date: 3 December 1965
Place: CS/TA Laboratory, USAECOM
Fort Monmouth, New Jersey
Organizations Represented:

Goodyear Aerospace (Arizona)

J. Fredlund
L. L. Schoenfeld
J. E. Winter

CS/TA Laboratory
Fort Monmouth, New Jersey

S. Graveline
Dr. L. Hatkin
O. E. Rittenbach

Purpose: Initial program conference; to review contract and technical specifications.

Date: 20 January 1966

Place: Goodyear Aerospace Corporation
Litchfield Park, Arizona

Organizations Represented:

Goodyear Aerospace (Arizona)

CS/TA Laboratory
Fort Monmouth, New Jersey

L. L. Schoenfeld

S. Graveline

Purpose: To review program status.

3. PROGRAM FOR THE NEXT INTERVAL

Plans for the second quarter include work in three basic areas. These are:

1. Completion of circuit design and demonstration of a complete system bread-board
2. Investigation of techniques to allow 30-minute storage time for the range versus azimuth storage-display tube
3. Packaging studies, including fabrication of an equipment mockup.

In addition, the azimuth portion of the radar target simulator will be developed. Effort will also be expended on study of integration techniques.

Security Classification

DOCUMENT CONTROL DATA - R&D		
(Security classification of title, body of abstract and indexing annotation must be entered when the overall report is classified)		
1. ORIGINATING ACTIVITY (Corporate author) Goodyear Aerospace Corporation Arizona Division Litchfield Park, Arizona		2a. REPORT SECURITY CLASSIFICATION UNCLASSIFIED
		2b. GROUP
3. REPORT TITLE Automatic Detection and Display Equipment for Moving Target Indication (ADDEM)		
4. DESCRIPTIVE NOTES (Type of report and inclusive dates) First Quarterly Report, 9 November 1965 - 31 January 1966		
5. AUTHOR(S) (Last name, first name, initial) Schoenfeld, L. L.		
6. REPORT DATE July 1966	7a. TOTAL NO. OF PAGES 48	7b. NO. OF REFS 7
8a. CONTRACT OR GRANT NO. DA 28-043 AMC-01711(E) b. PROJECT NO. 1P6-20901-A-188-03-01 c. d.	8a. ORIGINATOR'S REPORT NUMBER(S) GERA-1118 8b. OTHER REPORT NO(S) (Any other numbers that may be assigned this report) ECOM-01711-1	
10. AVAILABILITY/LIMITATION NOTICES This document is subject to special export controls and each transmittal to foreign governments or foreign nationals may be made only with prior approval of Commanding General, U.S. Army Electronics Command, ATTN: AMSEL-HL-CT-R, Fort Monmouth, N.J.		
11. SUPPLEMENTARY NOTES	12. SPONSORING MILITARY ACTIVITY U.S. Army Electronics Command Fort Monmouth, New Jersey 07703 AMSEL-HL-CT-R	
13. ABSTRACT This is the first quarterly report documenting the development of an Automatic Detection and Display Equipment for Moving Target Indicator (MTI). The equipment will contain 10 range gated channels; each channel containing 10 bandpass filters to cover the audiospectrum. Moving target information will be displayed on "B" type and doppler displays. An investigation of active filters was undertaken and a preliminary configuration selected for test. This circuit makes use of integrated operational amplifiers. In addition, the S-plane pole position for all 10 bandpass filters was calculated. Effort was also expended on development of a +10,000-vdc power supply for the storage-display tube. A 10-kHz, solid-state inverter driving voltage multipliers and rectifiers was selected for test. A small variable transformer was also developed to provide highly efficient adjustment of voltages. An input voltage regulator was developed and, through use of a special configuration, a regulating efficiency of 95 percent was achieved. Other development work consisted of preliminary test of an integrator-threshold circuit and the target generator and doppler modulator portion of a radar simulator.		

14. KEY WORDS	LINK A		LINK B		LINK C	
	ROLE	WT	ROLE	WT	ROLE	WT
MTI Video Processing Range Gated Filtering Combat Surveillance Radars Clutter Filters Storage Tubes Doppler Displays						

INSTRUCTIONS

1. **ORIGINATING ACTIVITY:** Enter the name and address of the contractor, subcontractor, grantee, Department of Defense activity or other organization (*corporate author*) issuing the report.

2a. **REPORT SECURITY CLASSIFICATION:** Enter the overall security classification of the report. Indicate whether "Restricted Data" is included. Marking is to be in accordance with appropriate security regulations.

2b. **GROUP:** Automatic downgrading is specified in DoD Directive 5200.10 and Armed Forces Industrial Manual. Enter the group number. Also, when applicable, show that optional markings have been used for Group 3 and Group 4 as authorized.

3. **REPORT TITLE:** Enter the complete report title in all capital letters. Titles in all cases should be unclassified. If a meaningful title cannot be selected without classification, show title classification in all capitals in parenthesis immediately following the title.

4. **DESCRIPTIVE NOTES:** If appropriate, enter the type of report, e.g., interim, progress, summary, annual, or final. Give the inclusive dates when a specific reporting period is covered.

5. **AUTHOR(S):** Enter the name(s) of author(s) as shown on or in the report. Enter last name, first name, middle initial. If military, show rank and branch of service. The name of the principal author is an absolute minimum requirement.

6. **REPORT DATE:** Enter the date of the report as day, month, year, or month, year. If more than one date appears on the report, use date of publication.

7a. **TOTAL NUMBER OF PAGES:** The total page count should follow normal pagination procedures, i.e., enter the number of pages containing information.

7b. **NUMBER OF REFERENCES:** Enter the total number of references cited in the report.

8a. **CONTRACT OR GRANT NUMBER:** If appropriate, enter the applicable number of the contract or grant under which the report was written.

8b, 8c, & 8d. **PROJECT NUMBER:** Enter the appropriate military department identification, such as project number, subproject number, system numbers, task number, etc.

9a. **ORIGINATOR'S REPORT NUMBER(S):** Enter the official report number by which the document will be identified and controlled by the originating activity. This number must be unique to this report.

9b. **OTHER REPORT NUMBER(S):** If the report has been assigned any other report numbers (*either by the originator or by the sponsor*), also enter this number(s).

10. **AVAILABILITY/LIMITATION NOTICES:** Enter any limitations on further dissemination of the report, other than those

imposed by security classification, using standard statements such as:

- (1) "Qualified requesters may obtain copies of this report from DDC."
- (2) "Foreign announcement and dissemination of this report by DDC is not authorized."
- (3) "U. S. Government agencies may obtain copies of this report directly from DDC. Other qualified DDC users shall request through _____."
- (4) "U. S. military agencies may obtain copies of this report directly from DDC. Other qualified users shall request through _____."
- (5) "All distribution of this report is controlled. Qualified DDC users shall request through _____."

If the report has been furnished to the Office of Technical Services, Department of Commerce, for sale to the public, indicate this fact and enter the price, if known.

11. **SUPPLEMENTARY NOTES:** Use for additional explanatory notes.

12. **SPONSORING MILITARY ACTIVITY:** Enter the name of the departmental project office or laboratory sponsoring (paying for) the research and development. Include address.

13. **ABSTRACT:** Enter an abstract giving a brief and factual summary of the document indicative of the report, even though it may also appear elsewhere in the body of the technical report. If additional space is required, a continuation sheet shall be attached.

It is highly desirable that the abstract of classified reports be unclassified. Each paragraph of the abstract shall end with an indication of the military security classification of the information in the paragraph, represented as (T), (S), (C), or (U).

There is no limitation on the length of the abstract. However, the suggested length is from 150 to 225 words.

14. **KEY WORDS:** Key words are technically meaningful terms or short phrases that characterize a report and may be used as index entries for cataloging the report. Key words must be selected so that no security classification is required. Identifiers, such as equipment model designation, trade name, military project code name, geographic location, may be used as key words but will be followed by an indication of technical context. The assignment of links, rules, and weights is optional.